

Experimental test of visuomotor updating models that explain perisaccadic mislocalization

Sigrid M. C. I. Van Wetter

Radboud University Nijmegen,
Donders Institute for Neuroscience,
Department of Biophysics, Nijmegen,
The Netherlands



A. John Van Opstal

Radboud University Nijmegen,
Donders Institute for Neuroscience,
Department of Biophysics, Nijmegen,
The Netherlands



Localization of a brief visual target is inaccurate when presented around saccade onset. Perisaccadic mislocalization is maximal in the saccade direction and varies systematically with the target-saccade onset disparity. It has been hypothesized that this effect is either due to a sluggish representation of eye position, to low-pass filtering of the visual event, to saccade-induced compression of visual space, or to a combination of these effects. Despite their differences, these schemes all predict that the pattern of localization errors varies systematically with the saccade amplitude and kinematics. We tested these predictions for the double-step paradigm by analyzing the errors for saccades of widely varying amplitudes. Our data show that the measured error patterns are only mildly influenced by the primary-saccade amplitude over a large range of saccade properties. An alternative possibility, better accounting for the data, assumes that around saccade onset perceived target location undergoes a uniform shift in the saccade direction that varies with amplitude only for small saccades. The strength of this visual effect saturates at about 10 deg and also depends on target duration. Hence, we propose that perisaccadic mislocalization results from errors in visual-spatial perception rather than from sluggish oculomotor feedback.

Keywords: human, spatial perception, sensorimotor integration, efferent feedback, spatial accuracy, oculomotor system, visual system

Citation: Van Wetter, S. M. C. I., & Van Opstal, A. J. (2008). Experimental test of visuomotor updating models that explain perisaccadic mislocalization. *Journal of Vision*, 8(14):8, 1–22, <http://journalofvision.org/8/14/8/>, doi:10.1167/8.14.8.

Introduction

Three decades ago, Hallett and Lightstone (1976) demonstrated that a visual target, flashed in darkness before or during an intervening saccadic eye movement, is accurately localized by a subsequent saccade. As visual feedback cannot take this behavior into account, spatial accuracy results from remapping the target coordinates by feedback mechanisms that incorporate eye movements. It is now well established that the generation of goal-directed saccades involves efferent feedback and that the use of this extraretinal information underlies our ability to perceive a stable visual environment, despite the incessant occurrence of rapid eye movements that continuously shift the visual scene across the retina. This problem was first recognized by Von Helmholtz (1866).

Sparks and Mays (1983) showed that a planned saccade toward a briefly flashed target in darkness accounts for an unexpected intervening perturbation of eye position induced by micro-stimulation of the midbrain superior colliculus (SC). This experiment thus demonstrated that

the visuomotor system even has access to eye movement information when the animal is not planning the intervening saccade.

To explain accurate spatial behavior of saccades, the original control model of Robinson and colleagues (Van Gisbergen, Robinson, & Gielen, 1981) assumed that the efferent feedback signal was expressed as an *eye-position* signal that was used to construct a stable representation of visual targets in head-centered coordinates. However, later theoretical considerations about the role of the SC in saccade generation (e.g., Jürgens, Becker, & Kornhuber, 1981; Scudder, 1988) as well as a number of neurophysiological observations (see below) suggested that the visuomotor system employs *eye-displacement* signals to encode saccades and to perform the spatial updating. Thus, the updating mechanism is thought to operate in relative oculocentric coordinates rather than in absolute head-centered coordinates.

For example, recordings from saccade-related cells in the SC during both the double-step paradigm and the stimulation paradigm (Sparks & Mays, 1983) indicated that activity encodes the updated motor-error coordinates

of the second target and thus reflected the spatially correct saccade (Sparks & Porter, 1983). These recording experiments suggested that spatial updating occurs upstream from the SC, and that the remapping is based on eye-movement information generated at or downstream from the SC. Indeed, later experiments showed that visual activity of cells in posterior parietal cortex (Duhamel, Colby, & Goldberg, 1992), frontal eye fields (FEF; Umeno & Goldberg, 1997), and also the SC (Walker, Fitzgibbon, & Goldberg, 1995) carry the updated motor error signal even before the onset of a planned saccade, a phenomenon that has been termed *predictive remapping*. Recent evidence has indicated that FEF cells receive an efference copy of the saccadic eye movement that emanates from the saccade-related SC cells (Sommer & Wurtz, 2002, 2006).

However, despite the abovementioned accuracy of visuomotor behavior, a number of other studies have reported systematic localization errors associated with saccadic eye movements, starting with Martin and Pearce (1965). For example, Dassonville and colleagues showed that in a double-step trial the second saccade systematically mislocalizes a visual target when it was briefly presented around the primary saccade in darkness. They showed that the localization error was in the direction of the first saccade, and that the size of the error varied systematically with the target-saccade onset delay. Their data indicated that these errors could be as large as 70% of the first-saccade amplitude (Dassonville, Schlag, & Schlag-Rey, 1992, 1995; Schlag & Schlag-Rey, 2002).

Not only is a single point target mislocalized, also the allocentric visual information becomes distorted around a saccade. This was demonstrated in a vernier alignment task of visual dots by Cai, Pouget, Schlag-Rey, and Schlag (1997). In their experiment, the relative retinal locations of the dots were perceived differently when a brief probe dot was flashed near saccade onset between two permanently illuminated dots.

Perisaccadic mislocalization of stimuli has also been demonstrated by a number of perceptual experiments in the light, and alternative theories to explain visual perceptual stability under these conditions have been forwarded. For example, Bridgeman, Van der Heijden, and Velichkovsky (1994) and Deubel, Bridgeman, and Schneider (1998) proposed that in the light perceived visual stability might be entirely due to visual processing, as the saccade target could serve as a special reference object for the perceptual system. Their hypothesis holds that the visual properties of the saccade target are stored in memory before saccade initiation. As long as the postsaccadic target properties are the same as the memorized properties, the scene is perceived as stable. Extraretinal information about the saccade would be required only in case of a mismatch in the comparison (e.g., under open-loop localization conditions, when the postsaccadic target is absent).

In line with the saccade-target theory, Ross, Morrone, and Burr (1997) provided evidence that visual space becomes compressed toward the saccade endpoint, briefly before the occurrence of a saccade across a visual background. Awater, Burr, Lappe, Morrone, and Goldberg (2005) recently extended the experiments of Ross et al. by studying visual compression for adapted saccades. They found that compression was determined by the actual, adapted saccade, rather than by the intended, nonadapted eye movement. Awater and Lappe (2006) and Lappe, Awater, and Krekelberg (2000) argued that visual compression results from a *postsaccadic* analysis by the perceptual system. According to their proposal, presaccadic retinotopic and allocentric target relations are compared with the visual situation immediately after the saccade and is combined with eye-movement information from that saccade for evaluation.

Visuomotor updating models

To yield spatially accurate behavior under open-loop conditions, the visuomotor system has no choice but to combine retinal and extraretinal information; the latter is thought to be the saccadic displacement signal (see above). An accurate representation of the oculocentric location of the second visual target in a double-step trial (T_E) is then determined by

$$T_E = T_{R2} - S_1, \quad (1)$$

where T_{R2} is the initial retinal location of the second target, and S_1 is the intervening saccadic eye displacement toward the first target in the trial. Since the perceptual system relies on neural representations of these variables, the reconstructed, or perceived, oculocentric target is

$$T_E^P = T_{R2}^P - S_1^P \quad (2)$$

in which T_{R2}^P and S_1^P are the internal representations of the (memorized) retinal target location and eye displacement. Clearly, a localization error occurs whenever either of these signals is not veridical, as in that case $T_E^P \neq T_E$.

Dassonville and colleagues explained their data with a model in which the eye-movement feedback is a sluggish version of the actual oculomotor command (Dassonville et al., 1992, 1995; Honda, 1990, 1991; Schlag & Schlag-Rey, 2002).

Their model is conceptualized in Figure 1A (“oculomotor model”). At the time of the flash (presented at delay, t_0 , with respect to saccade onset), the perceived eye movement, $S_1^P(t_0)$, differs from the actual eye displacement, $S_1(t_0)$. This difference gives rise to a localization error in the direction of the saccade, which varies systematically with the flash delay (Figure 1D, “fast”).

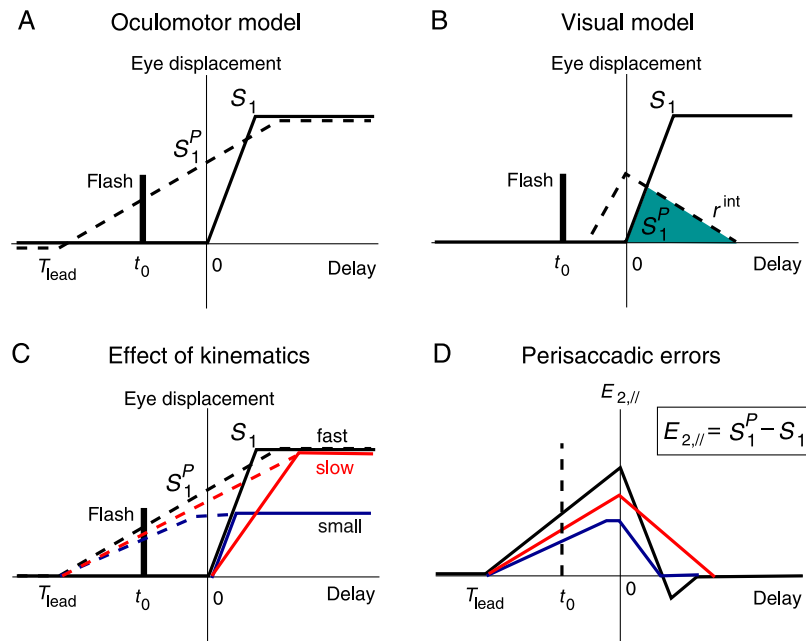


Figure 1. Different visuomotor updating models to explain mislocalization of a flashed target, given at time t_0 , around the onset of saccade S_1 . (A) The oculomotor model assumes a correct visual signal, but a sluggish internal eye-movement signal, S_1^P (dashed line; T_{lead} : lead time). (B) The visual model assumes a correct extraretinal signal, S_1 , but a delayed and filtered representation of the flash, r^{int} . Perceived eye displacement is the weighted average of S_1 over the shaded interval. (C) The perceived extraretinal signal (here, for the oculomotor model) depends on saccade amplitude and kinematics. (D) Consequently, error patterns as function of flash delay vary with amplitude and kinematics of S_1 .

Note that toward the end of the saccade the error may even reverse sign (Honda, 1991).

Pola (2004) argued that an extremely brief stimulus (few ms) is actually a poor temporal probe to localize a target, as it produces persistent activity in the visual pathway. This prolonged activity may be described by a delayed and low-pass filtered representation of the brief retinal pulse (Figure 1B, r^{int}). In his visual model, the dispersed visual activity is used to estimate current eye displacement by taking a temporal average, which leads to an error in the perceived eye displacement. Pola (2004) pointed out that such a mechanism could explain the observed perisaccadic errors equally well (“visual model,” Figure 1B).

According to Ross et al. (1997), errors in the perceived target location in structured visual environments result from combined errors in the presaccadic visual and oculomotor representations. They proposed that around a saccade, the representation of the visual field is compressed toward the saccade endpoint. Since both the visual and the oculomotor representations deviate from their actual values, the spatial location of the target will be misjudged too.

It is important to note that regardless the cause of perisaccadic mislocalization (visual spatial compression, visual temporal dispersion, or a sluggish eye movement), all abovementioned models predict that the error will depend on the primary-saccade amplitude and on its kinematics. This point is illustrated for the oculomotor

model in Figures 1C and 1D for the case of a small, a large, and a slow saccade. The small saccade produces smaller localization errors than the large saccade, but the same is true for the slow saccade when it is compared to the fast saccade with the same amplitude.

The present study investigates and tests the predictions of the visuomotor updating models for a large range of first-saccade properties in double steps executed to briefly flashed point targets in complete darkness. To our knowledge, such an influence has not been investigated so far. The only study to date is by Ostendorf, Fischer, Finke, and Ploner (2007), who demonstrated a correlation between intersubject variability in saccade peak velocities and the strength of visual compression in a perceptual paradigm similar to that of Ross et al. (1997).

In the Results section, we will first present extensive simulations, in which model saccades were used to precisely quantify the predictions of the different visuomotor updating schemes. These simulations show that the influence of saccade kinematics on the localization error is strongly modulated by the timing of the target flash. Interestingly, this modulation is sensitive neither to the type of updating (motor, visual, visuomotor, or visual compression, see above) nor to the specific values of the parameters that define the visuomotor updating schemes.

We further report that although the predictions of the visuomotor updating models, when applied to real saccades, are very similar to the simulated results, they are not supported by our data. Instead, we show that the

observed error patterns are largely insensitive to the first-saccade properties. We propose an alternative explanation, according to which the perceived visual location of the target, $T_{R_2}^P$, undergoes a dynamic shift in the direction of the saccade. This uniform shift depends only weakly on the saccade amplitude, but not on target eccentricity. The resulting localization errors are thus mainly determined by the target onset delay and by visual target properties like its duration.

Methods

Subjects

Four male subjects, aged between 23 and 49 years, participated in the experiments. Subject JO is one of the authors; the other three subjects were naive regarding the purpose of this study. All subjects had normal binocular vision except for JO who is amblyopic in his right, recorded eye (visual acuity $>6/60$). Informed consent was obtained. Experiments adhered to the principles of the Declaration of Helsinki and the US federal regulations for the Protection of Human Subjects.

Apparatus

Experiments were conducted in a completely dark room ($W \times L \times H = 2.5 \times 3.5 \times 2.5 \text{ m}^3$), in which two pairs of $2.5 \times 2.5 \text{ m}^2$ coils were attached to the left/right walls and floor/ceiling to generate the horizontal (30 kHz) and the vertical (40 kHz) magnetic fields needed for the scleral search coil technique (Robinson, 1963). The subject was seated in a chair with his head in the center of the magnetic fields and firmly supported by a head and neck rest to prevent head movements.

Visual stimuli were provided by green light-emitting diodes (LEDs; $\lambda = 568 \text{ nm}$; Knightbright Electronics, L59EGW/CA; diameter 2.5 mm, corresponding to 0.2 deg viewing angle). The LEDs were powered with current pulses (frequency 150 Hz) and set to a relatively low intensity of 0.56 cd/m^2 (calibrated with a Minolta LS-100 luminance meter).

To measure eye movements, the subject wore a search coil (Skalar Instruments, Delft, The Netherlands; Collewijn, van der Mark, & Jansen, 1975) on his right eye. Horizontal and vertical components of eye movements were extracted from the coil signal by lock-in amplifiers (Princeton Applied Research, model 128A) that were tuned to the respective field frequencies, low-pass filtered with a 4th order low-pass anti-aliasing filter (cut-off at 150 Hz) and amplified with a custom-made amplifier. Signals were subsequently digitized at a sample frequency of 500 Hz/channel (Metrabyte, DAS-16) and stored on hard disk for

further off-line analysis. Stimulus generation and data acquisition were controlled by a PC 486 that was equipped with a timer board (National Instruments, DT2817) and an I2C board to control the LEDs.

LEDs ($n = 85$) were mounted on a thin-wire hemisphere with a radius of 0.85 m. The LEDs were mounted at 7 different polar coordinate eccentricities, R , and directions, Φ , with respect to the straight-ahead central LED ($[R, \Phi] = [0,0] \text{ deg}$) at $R \in [2, 5, 9, 14, 20, 27, 35] \text{ deg}$, and $\Phi \in [0, 30, 60, \dots, 330] \text{ deg}$, where $\Phi = 0$ is rightward, and $\Phi = 90$ deg is upward with respect to the central LED.

Paradigms

Calibration

Each experimental session started with a calibration run to obtain steady fixations of the eye at all LED positions. Each trial started with fixation of the central LED for 600–800 ms. When this LED was extinguished, a peripheral LED, pseudo-randomly selected from one of 72 locations, was illuminated for 1.0 s (the innermost LEDs at $R = 2 \text{ deg}$ were not used). The subject was required to make an accurate saccade to the peripheral LED and to maintain fixation as long as it was illuminated. During calibration, the visual stimuli had an intensity of about 1.0 cd/m^2 .

Double-step paradigms

Default double-step trial

In the default double-step paradigm, the initial fixation position was pseudo-randomly selected from $[R_0, \Phi_0] = [2,0]$ or $[2,180] \text{ deg}$ and presented for 600–1000 ms. The subject had to foveate this fixation spot. When this spot extinguished, the first visual target (0.56 cd/m^2) would appear after a 100-ms gap of darkness for a duration of 20 ms at either $[R_1, \Phi_1] = [14,0]$ or $[14,180] \text{ deg}$, with respect to straight ahead, i.e., at a retinal eccentricity of $R \in [12,16] \text{ deg}$ left or right from the initial fixation point. The subject had to make a saccade to this stimulus as fast and as accurately as possible.

In 90% of the trials, a second visual target (0.56 cd/m^2) would be presented for 15 ms. The onset of this stimulus was pseudo-randomly selected from $\Delta T \in [80, 100, \dots, 240] \text{ ms}$ after the offset of the first stimulus to ensure an approximately homogeneous distribution of stimulus delays relative to the first-saccade onset (which typically had a latency of about 200 ms). This second stimulus could be presented at either one of six different locations, pseudo-randomly selected from $[R_2, \Phi_2] = [20, 60], [14, 90], [20, 120], [20, 240], [14, 270],$ or $[20, 300] \text{ deg}$, with respect to straight ahead, and creating a variation in retinal target locations. In these trials, the subject was required to refixate also the perceived location of the second visual stimulus as fast and as accurately as possible.

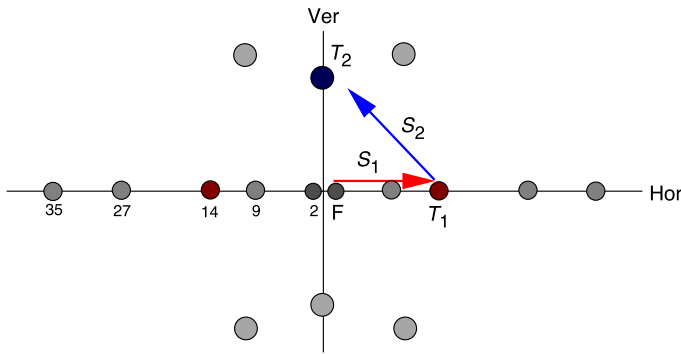


Figure 2. Target configuration for the double-step saccade experiments in the amplitude series. The initial fixation point (F) is presented at either two deg right or left from straight-ahead. The first target in the double-step is at a fixed eccentricity (left or right) from straight-ahead, either at 9, 14, 27, or 35 deg. Six different locations serve for the brief second target flash, T_2 , which is presented around the onset of S_1 , the first-saccade response to T_1 . The highlighted example shows the default amplitude experiment ($T_1 = 14$ deg), with T_2 flashed at the 14-deg upward location.

All subjects participated in seven different double-step recording sessions: (i) Four *amplitude* sessions in which the first saccade was always horizontal, but the eccentricity of the first stimulus was different in each session: $R_1 \in [9, 14, 27, 35]$ deg re. straight ahead, $\Phi_1 \in [0, 180]$. Figure 2 shows the spatial distribution of stimuli in the experiments. (ii) One *direction* session in which the amplitude of the first saccade was kept at $R_1 = 14$ deg, but its direction was varied pseudo-randomly from $\Phi_1 \in [60, 210, 330]$ deg (here, the second target at (20,60) deg was replaced by (20, 30) deg); and (iii) two *duration* sessions in which the first target was horizontal at an eccentricity of 14 deg, but the duration of the second target was either 5 or 50 ms.

In a typical recording session, two to four double-step runs, each consisting of 116 double-step trials and 14 single-step catch trials, were performed.

Visuomotor updating models

Several visuomotor updating models have been proposed to account for the dynamic pattern of perisaccadic localization errors in the double-step paradigm. All models have in common that the errors arise as a result of errors in the visuomotor transformation that updates the initial retinal target coordinates with an efference copy of the oculomotor command:

$$\vec{T}_2(t_0) = \vec{R}_2(t_0) - \Delta\vec{S}_1(t_0), \quad (3)$$

with $T_2(t_0)$ the location of the flashed target in oculocentric coordinates, $R_2(t_0)$ is the retinal error vector of the

target at the time of the flash, and $\Delta S_1(t_0)$ is the eye displacement of the primary saccade following the target flash at time t_0 (e.g., Vliegen, Van Grootel, & Van Opstal, 2004, 2005).

Model 1: Oculomotor model

In the model proposed by Dassonville et al. (1992), localization errors arise because of a discrepancy between the actual eye displacement at time t , $S(t)$, and the perceived eye displacement at time t , which is the extraretinal signal $S^P(t)$. The latter is supposed to lead the former by ΔT_{lead} , about 160 ms, but the representation of its trajectory is a low-pass filtered version of the actual trajectory:

$$S^P(t) = \int_0^{\infty} S(t + \Delta T_{\text{lead}} - \tau) \cdot h_s(\tau) d\tau, \quad (4)$$

where the LP filter (time constant T_s , and order n_s) is described by

$$h_s(\tau) = \frac{\tau^{n_s-1}}{(n_s-1)!} \cdot e^{-\tau/T_s}. \quad (5)$$

A localization error arises because the internal update process is determined by

$$\vec{T}_2^P(t_0) = \vec{R}_2(t_0) - \Delta\vec{S}_1^P(t_0), \quad (6)$$

and because the total saccade vector $\vec{S}_1 \equiv \vec{S}_1(t) + \Delta\vec{S}_1(t)$, it follows that the expected error is in the direction of the first saccade, given by

$$E_{2, //}(t_0) = S_1^P(t_0) - S_1(t_0), \quad (7)$$

which is the difference between perceived and actual eye displacements at the time of the flash.

Models 2 and 3: Visual and visuomotor models

Pola (2004) argued that the perisaccadic localization errors in the double-step paradigm may have a visual, rather than an oculomotor, origin. The probe stimulus, R_2 , which is presented for a very brief time, is in fact temporally smeared (i.e., LP filtered) within the visual system. As a result, the visual-perceptual system, which uses this blurred visual input to sample the internal eye-movement signal, has no precise information about eye displacement at the time of the flash. The visual probe stimulus R_2 (duration D_v ms, presented at $t = t_0$) gives rise to a temporally LP filtered version of the visual pulse. Thus, although the retinal stimulus can be described

as $\vec{R}_2(t) = r(t) \cdot \vec{R}_2$ with $r(t)$ the temporal retinal activation:

$$r(t) = \begin{cases} 1 & \text{for } 0 \leq t - t_0 \leq D_v, \\ 0 & \text{otherwise} \end{cases}, \quad (8)$$

the resulting visual activity is delayed by ΔT_{lag} and is given by

$$r^{\text{int}}(t, t_0) = \int_0^{\infty} r(t - t_0 - \Delta T_{\text{lag}} - \tau) \cdot h_v(\tau) d\tau, \quad (9)$$

with the temporal visual filter:

$$h_v(\tau) = \frac{\tau^{n_v-1}}{(n_v-1)!} \cdot e^{-\tau/T_v}. \quad (10)$$

Note that this filter characteristic might also depend (in an as yet unknown way) on the properties of the visual stimulus, such as its duration, intensity, contrast, size, shape, and color. In our simulations, we took a fixed characteristic.

According to the *visual model*, the internal representation of eye displacement is accurate, apart from a short delay of up to a few tens of ms, thus $S^{\text{int}}(t) = S(t - \Delta T_{\text{delay}})$.

In a more general version of this conceptual idea, both the visual input and the oculomotor feedback signals are low-pass filtered versions of the actual signals. This idea combines [Equations 9 and 4](#) (albeit with different parameter values to account for the observed error patterns, see [Results](#) section and [Table 1](#)) and will be termed the *visuomotor* model.

In the visual and visuomotor models of [Pola \(2004\)](#), the perceived eye displacement at the time of the target flash

Model	ΔT_{del}	n_v	T_v	ΔT_{lead}	n_s	T_s
Motor	1	1	1	-160	2	5
				-130	5	10
				-100		20
Visual	20	2	5	-20	1	1
		5	10	+10		
			20	+40		
Visuomotor	30	2	5	-60	2	5
			10	-40	5	10
			20	-20		20

Table 1. Parameter ranges used to simulate perisaccadic localization errors with three of the visuomotor updating models described in the [Methods](#) section. Twelve parameter sets were selected for each of the models. See [Figures 4B and 6](#) for results. The default values for each model are highlighted in bold.

is determined by the weighted temporal average of the internal visual and oculomotor signals ([Pola, 2004](#)):

$$S^P(t_0) = \int_0^{\infty} r^{\text{int}}(t, t_0) \cdot S^{\text{int}}(t) dt. \quad (11)$$

Because this weighted averaged eye-displacement signal differs from the actual eye displacement, a discrepancy arises, which again, through [Equation 6](#), gives rise to a localization error.

Note that in the purely visual version of [Equation 11](#), the perceived eye movement differs from the internal eye displacement as a result of visual blurring only (as if measuring position with a moving camera). Thus, if the sensory stimulus would be *auditory*, this effect would be absent (or at least it would be different, see e.g., [Binda, Bruno, Burr, & Morrone, 2007](#); [Vliegen et al., 2004](#)). This contrasts with the oculomotor proposal of [Equation 4](#), for which the stimulus modality is immaterial.

Model 4: Visual compression model

The model proposed by [Ross et al. \(1997\)](#) combines oculomotor and visual effects: (i) It uses a sluggish version of the extraretinal eye-movement signal (described by the difference between a slowly rising offset eye position, $E^{\text{int}}(\text{end})$, and a slowly decaying onset eye position, $E^{\text{int}}(\text{start})$), that is, however, unrelated to the actual main sequence properties of saccades, and (ii) it introduces a *spatial* visual-field effect, in which the visual input undergoes a nonuniform, eccentricity-dependent nonlinear compression towards the fovea. The combination of these two effects leads to a distorted representation of the target in oculocentric coordinates, $\vec{T}_2^P(t_0)$ (cf. [Equation 6](#)), which is now expressed as

$$\vec{T}_2^P(t_0) = C(T(t_0)) \cdot \vec{R}_2(t_0) - \Delta \vec{S}_1^P(t_0). \quad (12)$$

In this formulation, $C(T)$ is the (dynamic) visual compression factor that depends in a nonlinear way on the instantaneous retinal location of the stimulus during the saccade, $T(t)$, and on the difference between the extra-retinal and actual eye-displacement signals:¹

$$C(T(t)) = \exp\left(-k \cdot \left| \frac{T(t) \cdot [S_1^P(t) - S_1(t)]}{S_1^2} \right|^\beta\right). \quad (13)$$

The dynamic retinal error of the target is defined by $T(t) = R_2 - S_1(t)$, where R_2 is the initial retinal location and $S_1(t)$ is the actual saccade. The extraretinal eye-displacement signal is given by $S_1^P(t) = E_1^{\text{int}}(\text{end}) - E_1^{\text{int}}(\text{start})$. Further, $k = 1.48$ and $\beta = 1.35$ are dimensionless constants

(for details, see Ross et al., 1997). Note that when the extraretinal signal is accurate, $C(T) = 1$, and there will be no localization error. Therefore, also this model predicts that perisaccadic localization errors will scale with the primary-saccade metrics and kinematics (see Results section and Figure 5C). In contrast to the other three models, however, the error will also systematically depend on the retinal eccentricity of the target probe (i.e., on the dynamic motor error of the target; see also below).

Simulated saccades

To investigate the theoretical predictions of the different visuomotor updating models captured by (Equations 4–13) (see Results section and Figures 4, 5, and 6), model saccades were generated by a simplified version of Robinson’s local feedback model (Van Gisbergen et al., 1981). To that end, the instantaneous eye displacement, $S(t)$, evoked by a step displacement on the retina of the stimulus location, R , was computed by

$$S(t) = m_0 \ln \frac{A \cdot \exp(v_{pk}t/m_0)}{1 + A \cdot \exp((v_{pk}t - R)/m_0)} \quad (14)$$

with $A \equiv \frac{1}{1 - \exp(-R/m_0)}$,

in which the parameters m_0 and v_{pk} determine the main sequence nonlinearity of the brainstem burst generator (BG) for eye velocity, $V(t)$:

$$V(t) = v_{pk} \cdot (1 - \exp(-T(t)/m_0)). \quad (15)$$

Here, $T(t) = R - S(t)$ is the dynamic retinal error (or dynamic motor error) that also figures in Equation 13.

To generate model saccades with varying amplitudes and kinematics (typically, $N = 500$), the characteristic of the BG was varied over a considerable range (v_{pk} drawn at random from the [300–750] deg/s interval, m_0 fixed at 7 deg), while the model produced horizontal saccades, randomly selected between [5 and 40] deg. Three different flashed target locations were chosen (as in our experiments), with (horizontal) initial retinal locations at $T_2 \in [-10, 0, +10]$ deg.

Then, for each saccade, the different models were applied to compute the internal representation of the eye-displacement signal that is used for the oculocentric target update. The resulting perisaccadic localization error was computed for 51 stimulus delays relative to the saccade onset (t_0 from -250 to $+250$ ms, in 10-ms steps). Figure 4A shows an example of the resulting error patterns obtained for four different saccade amplitudes

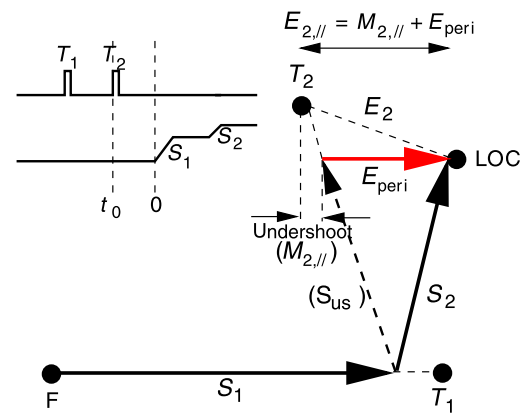


Figure 3. The double-step paradigm (inset). Saccade S_2 is directed toward LOC with overall error, E_2 . The error in the direction of saccade S_1 contains two contributions: one arising from the typical undershooting strategy ($M_{2,||}$, for planned saccade S_{us}) and the other, E_{peri} , resulting from perisaccadic mechanisms.

for Dassonville’s oculomotor model, set at the default eye-movement filter parameters.

In addition, the model simulations also incorporated the tendency of the oculomotor system to undershoot a visual target (see below, and Figure 3). To that end, we determined the motor error for the target at first-saccade offset and added an additional localization error of 10% of the motor error amplitude to the perisaccadic localization error to mimic this eccentricity-dependent undershoot.

Data analysis

Calibration and saccade selection

Data were calibrated off-line by mapping the end-fixations of the 73 fixation points from the calibration paradigm onto their known locations. The optimal parameters that map the digitized voltages onto known degrees of eye rotation were found by training two feed-forward neural networks for the horizontal and the vertical components of the eye-position signals, respectively (e.g., Vliegen et al., 2005). To calibrate the data, the neural networks were applied to the raw data samples. Saccades were detected in the calibrated data on the basis of acceleration and velocity criteria for their on- and offsets that could be separately set and adjusted by the experimenter. First-saccade responses with an onset latency of less than 80 ms or longer than 500 ms and with an amplitude less than half the motor error vector were excluded from the analysis. Second-saccade responses with latencies (relative to T_2) exceeding 600 ms, with amplitudes less than half the motor error vectors, and directional errors exceeding 45 deg were also excluded. Trials in which the first saccade was not followed by a valid second response were not considered in the analysis.

Typically, less than 5% of the data were excluded on the basis of these criteria.

Localization error

The data were analyzed in the following way. First, the measured localization error, E_2 , of the second saccade was defined as the difference between the target position and the end position of the second saccade (Figure 4).

To obtain the localization error in the direction of the first-saccade vector, we computed

$$E_{2, //} = \vec{E}_2 \cdot \hat{s}_1, \quad (16)$$

with \hat{s}_1 the unit vector along the first saccade and \cdot denoting the vectorial inner product. Note, however, that this localization error contains two contributions: (i) an

error due to a systematic (preprogrammed) saccadic undershoot in the direction of the motor error vector, M_2 , that is unrelated to the timing of the target, and (ii) the perisaccadic localization error in the direction of the saccade, E_{peri} , due to an error in the visual-motor remapping process (Figure 3). Hence,

$$E_{2, //} = E_{\text{peri}} + M_{2, //}. \quad (17)$$

The motor error in the direction of the first saccade is given by $M_{2, //} = \vec{M}_2 \cdot \hat{s}_1$ (cf. Equation 16). It is important to note that this contribution to the error primarily depends on the amplitude of the second saccade, as undershoots tend to be about 10% of the retinal error vector. However, since in our experiments an increase in the first-saccade amplitude also induces larger retinal errors for the second saccade (as targets were presented at fixed locations in space), a hidden correlation results between the first-saccade amplitude and the motor error for the second saccade and hence for the potential localization error of that saccade. We accounted for this potential “constant error” by incorporating the motor error of the second saccade as an independent variable in our multiple regression analysis described below.

Running averages

To visualize the average trend of the errors as function of the target onset delay, a running average was computed by convolving the errors, ranked according to t_0 , with a Gaussian filter (standard deviation 5 data points; total window width 30 points).

Residual error

Error data obtained from the amplitude series ($R_1 = 9, 14, 27, \text{ and } 35 \text{ deg}$) were pooled to determine a grand running average, $\overline{E_{2, //}}(t_0)$, as function of the flash delay t_0 . As will be explained in the Results section, the model predictions will be analyzed on the so-called *residual errors*. To obtain these, we removed the mean systematic trend in the data by subtracting the grand running average from each of the measured errors at the respective flash timing:

$$E_{2, \text{res}}(t_0) = E_{2, //}(t_0) - \overline{E_{2, //}}(t_0). \quad (18)$$

According to the visuomotor feedback models, these residual errors will contain systematic contributions arising from variability in the first-saccade properties (amplitude, S_1 , and mean eye velocity, V_1 ; see Results section), but also from the tendency of saccades to undershoot the target by a fraction of the motor-error vector, M_2 (Figure 3, see also above). To quantify and dissociate these potential contributions, we performed a

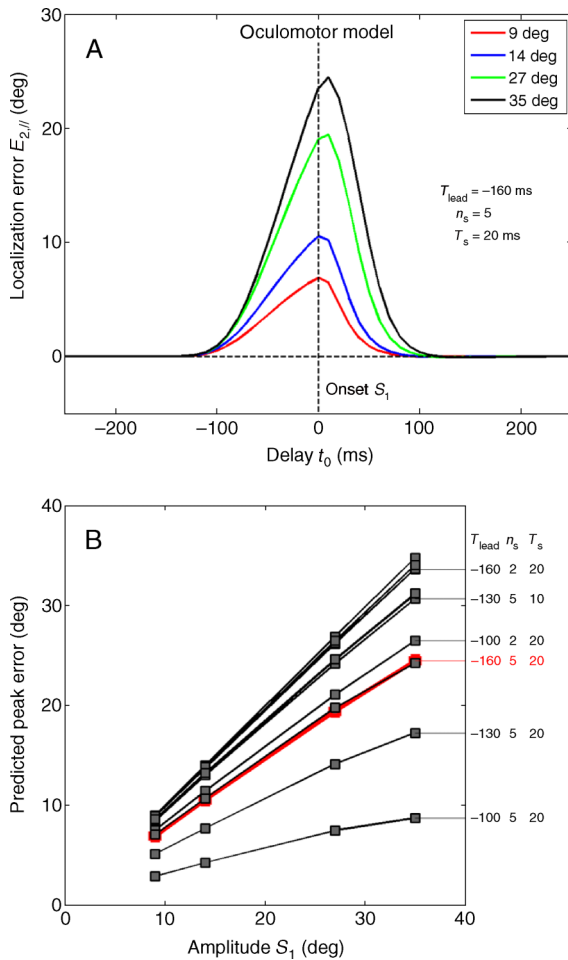


Figure 4. Simulation results for the oculomotor model. (A) Error patterns for four different saccade amplitudes, obtained with default parameter settings. (B) Peak localization error around saccade onset increases nearly linearly with first-saccade amplitude for all parameter settings. Red line: default parameters.

multiple linear regression on the residual errors according to

$$\hat{E}_{2,\text{res}} = a \cdot \hat{S}_1 + b \cdot \hat{V}_1 + c \cdot \hat{M}_{2,\text{//}}, \quad (19)$$

in which $\hat{X} \equiv (X - \mu_X)/\sigma_X$ is the normalized (dimensionless) variable (a.k.a. z-score, with X being either $E_{2,\text{res}}$, S_1 , V_1 , or $M_{2,\text{//}}$) and parameters $[a, b, c]$ are the dimensionless partial correlation coefficients.

We performed two regressions: The first analysis was done on the entire data set from the amplitude series pooled across the $[-250, +250]$ ms delay window around the first-saccade onset. In the second analysis, the regression was performed within 100-ms wide time bins that were shifted in 10-ms steps along the $[-250, +250]$ interval, with centers running from $[-200, +200]$ ms (i.e., 41 regressions with 90 ms overlap; e.g., Figure 5B). In this latter analysis, the temporal dynamics of the partial correlation coefficients for amplitude and mean velocity of the first saccade, $a(t_0)$, $b(t_0)$, and $c(t_0)$, were thus determined (for an illustration of this procedure, see Results section and Figure 5).

Predicted errors

The same analysis was run on simulated perisaccadic errors. To that end, we ran the different visuomotor updating models on our eye-movement data to verify whether the parameter values for the retinal stimulus filter, the eye-movement filter, or the combination of both, were critical for our results.

Since the models make equivalent predictions (see Results section and Figures 4, 5, and 6), we only report on the results obtained with the sluggish eye-movement feedback model to generate the predicted localization errors, as the implementation of this model is the most straightforward. To that purpose, we filtered each measured eye-movement trajectory to the first target, $S_1(t)$, with an LP filter. The parameters of this filter were chosen such that it yielded satisfactory predictions for the 14-deg amplitude experiments, i.e., a peak error of about 9 deg (see Results section). The impulse response of this filter is given by Equation 5.

The filtered eye-movement trajectory is then determined by the convolution of Equation 4. We took $T_s = 20$ ms, the filter's time constant, $n_s = 5$ as the order of the filter, and the lead time of the internal eye movement signal had a value of $\Delta T_{\text{lead}} = -160$ ms.

This procedure yielded the model's internal representation of the eye-movement trajectory, $S_1^P(t)$, for each measured saccade, $S_1(t)$. According to the oculomotor model, the expected error for each trial is then determined by the difference between perceived and actual eye displacements at the time of the flash (Equation 7; Figure 1D) and is given by Equation 4.

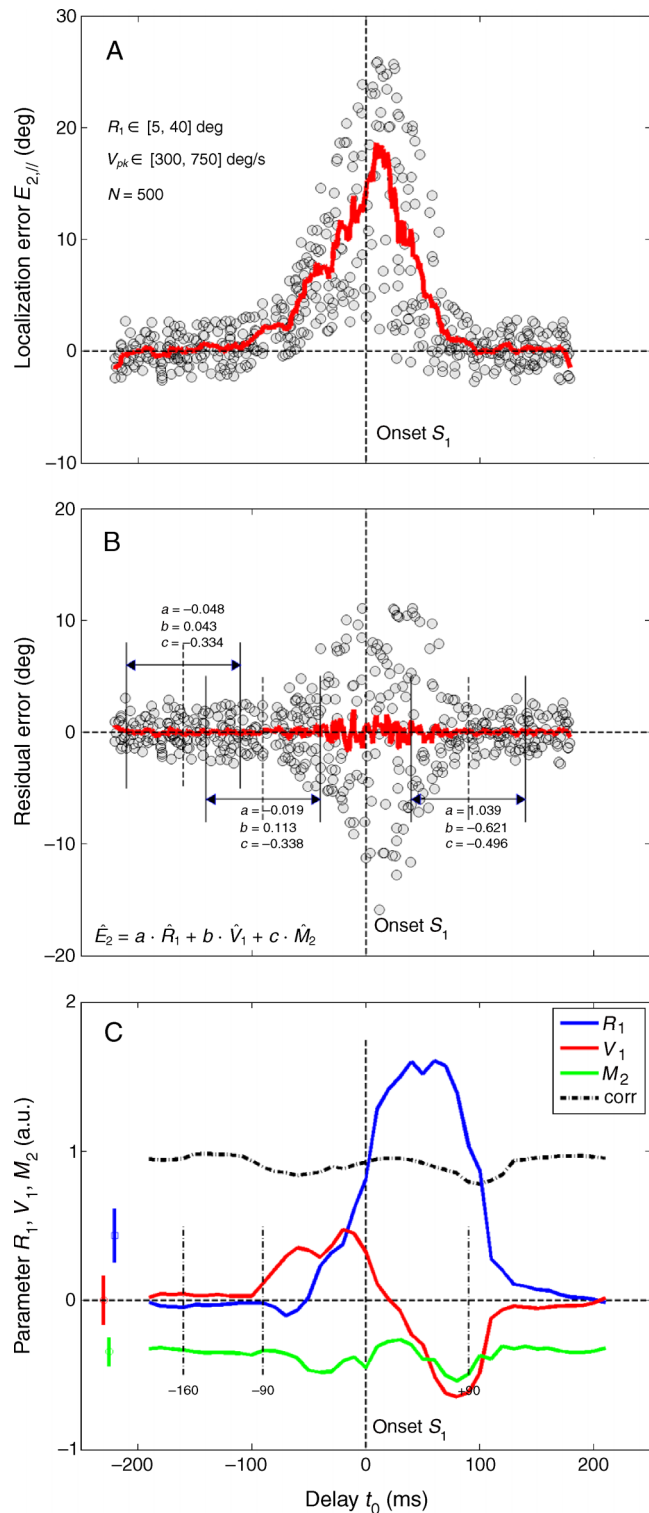


Figure 5. Different steps in the analysis to determine the influence of first-saccade amplitude, velocity, and motor error to target mislocalization, illustrated for simulated responses. (A) Raw error patterns as function of stimulus delay. Red line: running average. (B) Residual errors after removing the running average. Three 100-ms epochs are indicated with regression parameters. (C) Parameter dynamics for all delays. Vertical dotted lines correspond to the three epochs in panel B.

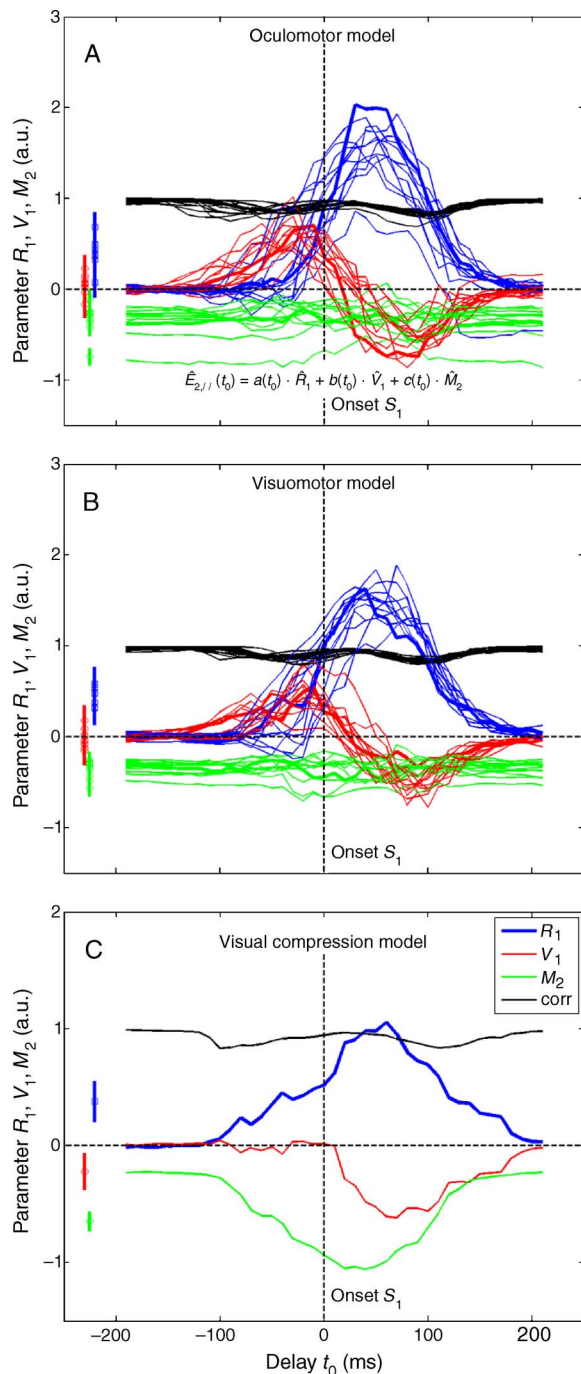


Figure 6. Dynamic parameter behavior of the multiple linear regression relation (Equation 19) for three different visuomotor updating models. Models were run with twelve different parameter sets (Table 1). (A) Oculomotor model (Dassonville et al., 1992). (B) Visuomotor model (Pola, 2004). Similar results were obtained for the visual model (data not shown). (C) Visual compression model (Ross et al., 1997) tested only with its published parameters. Note that the dynamic relations are very robust and quite similar for the different updating schemes. Note also that the influence of motor error differs for the compression model. Legend: R_1 : amplitude of first saccade; V_1 : mean eye velocity of first saccade; M_2 : motor error for second saccade; corr: correlation of the multiple regression.

The resulting pattern of simulated errors was subsequently subjected to the same regression analysis as the measured errors (Equation 19).

Results

Simulated saccades

To illustrate the rationale of our analysis, we will first investigate the predictions made by the four different models described in the Methods section. Figure 4 shows the results of simulations with the sluggish oculomotor feedback model (Equations 4–7), applied to fast saccades generated with a simple Robinson’s saccade model (Equations 14 and 15; $v_{pk} = 700$ deg/s). In Figure 4A, the perisaccadic localization errors are shown for four different amplitudes ($S_1 = [9, 14, 27, 35]$ deg) and default parameters of the oculomotor model. Note the clear increase of the errors as function of the saccade amplitude. The peak error is reached around the saccade onset and amounts about 65% of the saccade amplitude.

To investigate how the error patterns depend on the filter characteristics of the internal eye-displacement signal, we ran the model for 12 different parameter sets (Table 1). Figure 4B shows the relation between peak localization error as function of saccade amplitude. Parameter values for a number of cases are indicated next to the respective peak-error value. For all parameter sets, the peak error increases approximately linearly with the saccade amplitude. The slope of the relation depends on the parameters. Compare, for example, the default simulation (in red), for which $\Delta T_{lead} = -160$ ms, with the conditions with lead times of -130 and -100 ms, respectively: The longer the lead time, the larger the error. Also the effects of the filter parameters (filter order, n_s , and time constant, T_s) can be noted. For example, the lower the order and the shorter the time constant, the larger the error. The simulations with the visual and visuomotor models yielded very similar results (not shown, but see Figure 6). Table 1 provides a summary of the parameter ranges used in these simulations.

To compare the performance of the different visuomotor updating models across the entire flash-delay interval and to investigate the influence of the model parameters on their behavior, Figure 5 first illustrates our analysis for a complete simulation of the oculomotor model with default parameters.

In Figure 5A, the localization errors are shown for 500 simulated saccades, randomly selected over a large range of amplitudes and kinematics. As described in the Methods section, each error was further augmented by a 10% undershoot as determined from the motor error for the second saccade. This additional feature underlies the

scatter in the predicted errors for the long flash delays (below -120 ms and above $+100$ ms). The perisaccadic localization errors start to increase about -100 ms before the primary-saccade onset and reach their peak around the saccade onset, after which the errors rapidly decline back to baseline. To visualize the average trend in the data, the red solid line corresponds to the running average through the error data. Clearly, the errors are modulated not only by the timing of the flash, but also by the primary-saccade parameters (their amplitudes and eye velocity, see [Figure 1C](#)) and by the motor errors.

To quantify the influence of the latter three parameters, we removed the time-dependent trend in the data by subtracting the value of the running average at each corresponding data point. This resulted in so-called residual errors, which are shown in [Figure 5B](#). Because the perisaccadic localization errors increase with the saccade amplitude in a systematic way ([Figure 4](#)), the residual errors should reflect this dependence on the saccade parameters, predominantly within the interval where these errors occur. Indeed, the increased scatter within the flash-delay interval between -100 and $+100$ ms reflects this property of the perisaccadic errors.

To reveal the underlying relations, we performed the multiple linear regression analysis of [Equation 19](#) on the residual errors of [Figure 5B](#). Two analyses were performed: The first analysis was done on the entire data set. The parameter values (means and their standard error) of this analysis are shown in the left-hand side of [Figure 5C](#). This analysis shows a small positive partial correlation coefficient for the saccade amplitude, an insignificant coefficient for the mean eye velocity, and a negative coefficient for the motor error, the latter reflecting the consistent undershooting of the second saccades.

The second analysis was performed over 100-ms wide windows, which were shifted across the delay interval in 10-ms steps. [Figure 5B](#) highlights three of these intervals (centered around $t_0 = -160$, -90 , and $+90$ ms), together with the corresponding regression parameters. In this way, the analysis yields dynamic parameter estimates, $a(t_0)$, $b(t_0)$, and $c(t_0)$, respectively. The result of this analysis for the entire delay interval is shown in [Figure 5C](#). Now, a clear modulation of the primary-saccade parameters can be observed: The localization errors increase with saccade amplitude in the $[-100, +100]$ ms interval, as the dynamic parameter $a(t_0)$ is monophasic and positive. The influence of mean eye velocity is biphasic: It is positive before the initiation of the saccade and negative slightly after saccade onset, until after the saccade offset. The regression analysis also shows that the influence of motor error is negative, and roughly constant, throughout the flash-delay interval. This reflects the model's assumption that the preprogrammed saccadic undershoots are not related to the timing of the second target flash.

Considering that the size of the localization errors is strongly modulated by the model parameters ([Figure 4](#)), we assessed the sensitivity of these dynamic regression

relationships on the model parameters. We therefore repeated the complete analysis shown in [Figure 6](#) on all four versions of the visuomotor updating models. For the first three models, we performed the analysis for all twelve parameter sets. The visual compression model was run on the default parameters only ($k = 1.48$, $\beta = 1.38$, [Equation 13](#); see Ross et al., 1997). The results for three of the models are shown in [Figure 6](#).

It is immediately clear that all models produce essentially the same relationships for the influence of primary-saccade amplitude and kinematics. Moreover, the shape of the resulting relations is very robust and hardly influenced by the considerable variation in model parameter values ([Table 1](#)). Finally, the influence of motor error is the same for the three visuomotor updating models but differs qualitatively for the visual compression model.

This property of the latter model is caused by the influence of retinal target eccentricity on the perceived spatial location ([Equation 13](#)), which also induces a change of the programmed saccadic undershoot.

Results of the experiments

To validate our approach on the experimental data, it is necessary to demonstrate that (i) the variables of interest are broadly distributed to allow for meaningful regression analyses, (ii) subjects attempted to make goal-directed saccades under all test conditions, and (iii) our paradigm generated perisaccadic localization errors that reproduce the basic findings from the literature. In what follows, we will first assess these points.

Subjects participated in different double-step sessions in which we varied the eccentricity of the first visual target to elicit primary saccades with different amplitudes. To verify that the first-saccadic responses indeed covered a considerable range in both metrics and kinematics, [Figure 7](#) shows the distributions of the relevant variables for the pooled experiment of one of our subjects (RP). [Figures 7A](#) and [7B](#) show broad distributions of the horizontal components of the localization errors and motor errors for the second saccades. Note that the localization errors had a skewed distribution toward positive errors, indicating that, on average, errors tended to be in the same direction as the first saccade (see [Table 2](#)). [Figure 7C](#) shows the main-sequence relation for the primary saccades, which in the double-step paradigm tended to be less stereotyped than is usually reported for simple single-target saccades. Thus, a given amplitude of the primary saccade corresponds to a considerable range of mean eye velocities.

Despite substantial localization errors in the double-step experiments ([Figure 7A](#)), subjects typically performed well in the task, as the first- and second-saccade responses were goal directed. To quantify this, we determined overall localization performance by analyzing the first- and second-saccade responses for all trials (pooled for amplitudes) as function of their respective motor errors.

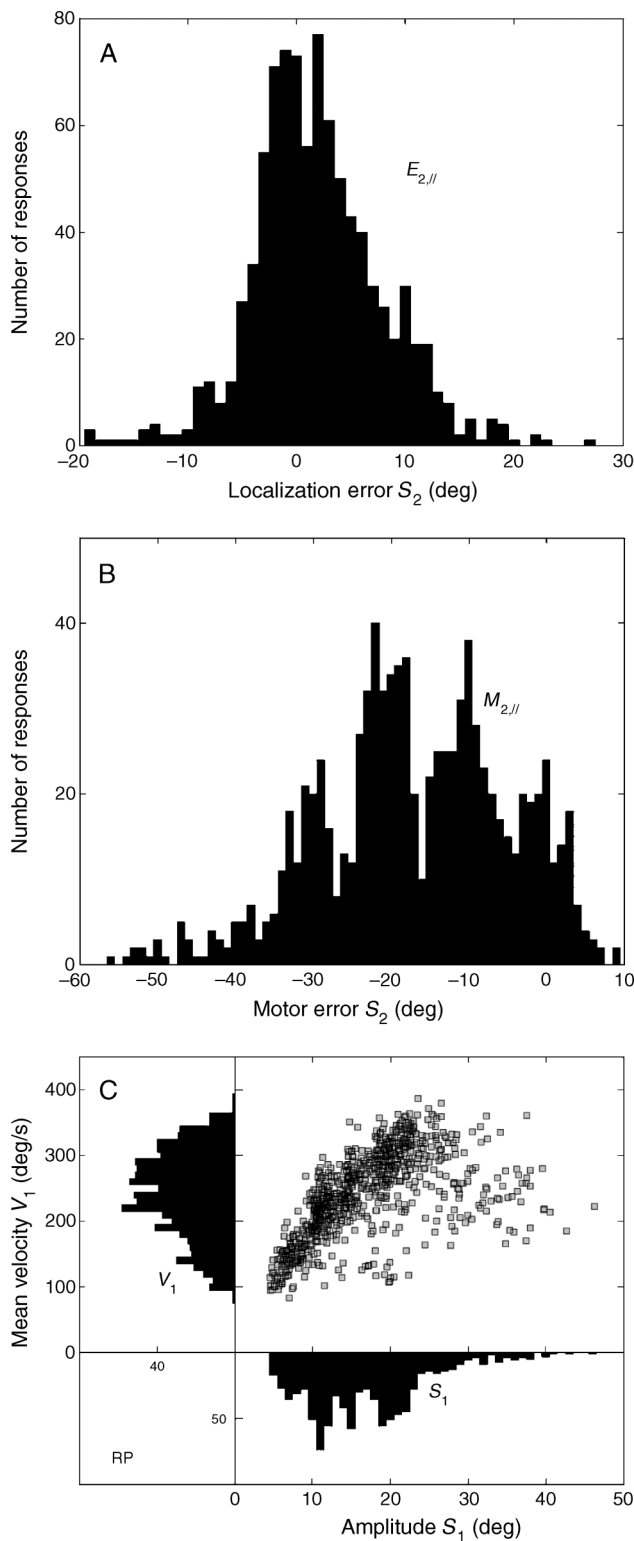


Figure 7. Distributions of localization errors of second saccades, measured in the direction of the first saccades (A), of the horizontal motor errors for the second saccades (B), and of the main-sequence properties of the primary saccades (C). Pooled data from subject RP ($N = 909$).

Figure 8 shows the horizontal components of the data for one representative subject (JO). Note that performance of the first-saccade responses (Figure 8A) was slightly better, as variability in the second saccades was typically somewhat larger (Figure 8B). Yet, the correlation between motor error and eye displacement was high, for both primary and secondary saccade responses ($R^2 = 0.97$ and 0.90 , respectively; $N = 1177$). The small variation in the initial fixation position (see Methods section) was accounted for in the primary saccades, which further indicates that subjects responded to the real retinal error signal, rather than to a potentially expected location. Yet, the slope of the linear regression lines tended to be lower for the secondary saccade responses, which reflects the systematic error of these responses into the direction of the primary saccade. Tables 2A and 2B provide a summary of the general response properties for the four subjects.

Finally, to demonstrate that the double-step paradigm (with a flash duration of 15 ms) yielded the pattern of

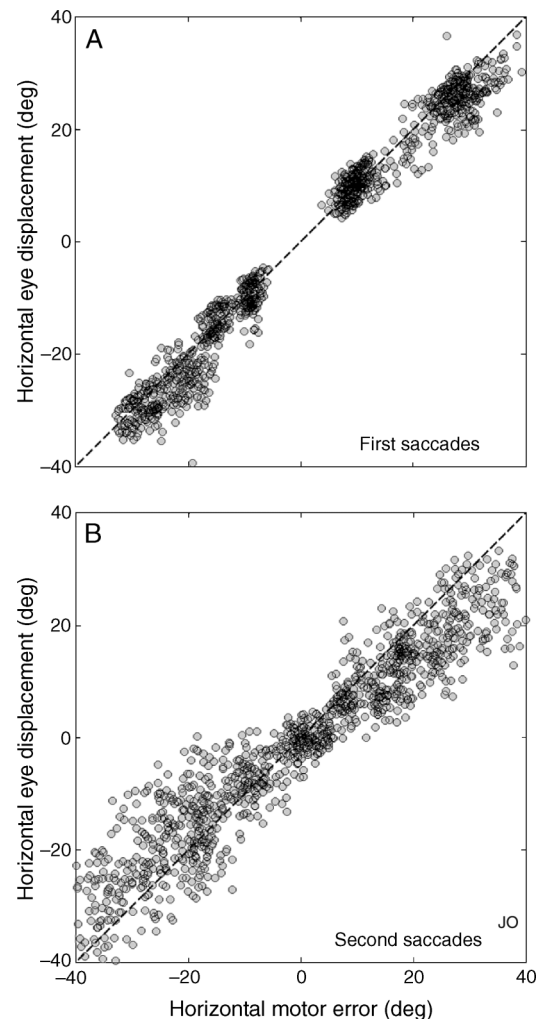


Figure 8. First (A) and second (B) saccade responses were goal directed. Pooled data from subject JO ($N = 1177$). Horizontal components only.

A	$E_{2, }$ (deg)	V_1 (deg/s)	$M_{2, }$ (deg)	S_1 (deg)	
JM	2.3 ± 5.6	244 ± 65	-16.6 ± 11.7	16.6 ± 7.8	
JO	4.8 ± 6.6	222 ± 51	-17.5 ± 11.8	19.4 ± 8.6	
RP	1.9 ± 6.1	241 ± 64	-16.9 ± 12.1	16.7 ± 7.4	
RW	1.2 ± 5.3	210 ± 60	-12.6 ± 10.7	13.2 ± 5.9	
B	a_1	r_1	a_2	r_2	N
JM	0.98	0.99	0.87	0.96	1031
JO	0.99	0.99	0.76	0.95	1177
RP	1.01	0.97	0.84	0.96	909
RW	1.01	0.99	0.61	0.94	626

Table 2. (A) Distributions of the saccade parameters. (B) Slope (a) and correlations (r) for first- and second-saccade responses.

perisaccadic errors that have been reported in other studies, Figure 9A shows the perisaccadic localization errors (Equation 16) as function of flash delay for the reference amplitude of $S_1 = 14$ deg (subject JM). Note that the errors started to increase between 150 and 100 ms before the saccade onset reached their peak of nearly 10 deg near the primary-saccade onset and then rapidly declined to zero during the saccade. The solid red line corresponds to the running average through the data (see Methods section). The black line corresponds to the prediction of the errors for the oculomotor model (Dassonville et al., 1992) with default parameters (see Figure 4A). Figure 9B shows the running averages for all four subjects. In all cases, the average peak error reached about 60% of the first-saccade amplitude, a value that is close to what has been reported before (Dassonville et al., 1992).

Effect of saccade amplitude on perisaccadic errors

To investigate whether the error patterns change in a systematic way with the primary-saccade amplitude, as predicted by the different visual-motor transformation models, Figure 10 shows the running averages obtained for the four amplitude series. Figure 10A depicts the curves obtained from the measured responses of subject JM.

Note that the data hint at a weak dependence of the errors on the first-saccade amplitude, as the peak errors tended to increase with amplitude for the smaller saccades. However, errors do not appear to exceed about 10 deg, whereas the visuomotor updating models predict a monotonic relationship (compare with Figure 4 for the oculomotor model predictions). Figure 10B shows the average errors for all four subjects as function of the first-saccade amplitude. The means and standard deviations were computed for the saccade responses within a 20-ms time bin around the peak error for each of the amplitude

series. Note that for all four subjects, the errors tend to saturate at a value of about 10 deg for the larger primary saccades. This is more clearly illustrated by the inset, which shows the interconnected means of the data for each subject.

To better quantify the differences between measured error patterns and the model predictions for the data and to assess the actual influence of the amplitude and the kinematics of the primary intervening saccade on the perisaccadic errors, we followed the quantitative analysis outlined in Figure 5. To that end, we first determined the residual errors for both the measured data set and the data set that would be predicted by the visuomotor updating models (Equation 18, for the pooled amplitudes). Since Figure 6 shows that the exact parameter sets of the different models hardly influence the sensitivity of the errors to the kinematic variables, we applied the oculomotor model with default parameters to the actual saccades (Equations 4–7) to predict the errors. Figure 11 shows the

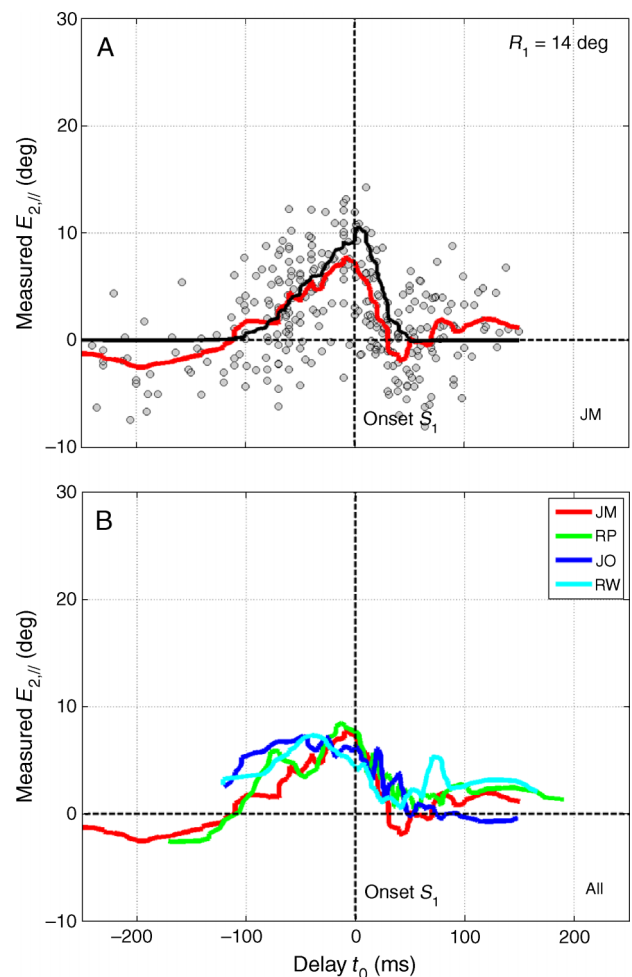


Figure 9. Localization errors for first saccades with an amplitude of about 14 deg. (A) Data from subject JM, with running average (red), and the prediction of the oculomotor model with default parameters (black; $\Delta T_{\text{lead}} = -160$ ms, $n_s = 5$, $T_s = 20$ ms, Equations 5 and 6). (B) Running averages for all four subjects.

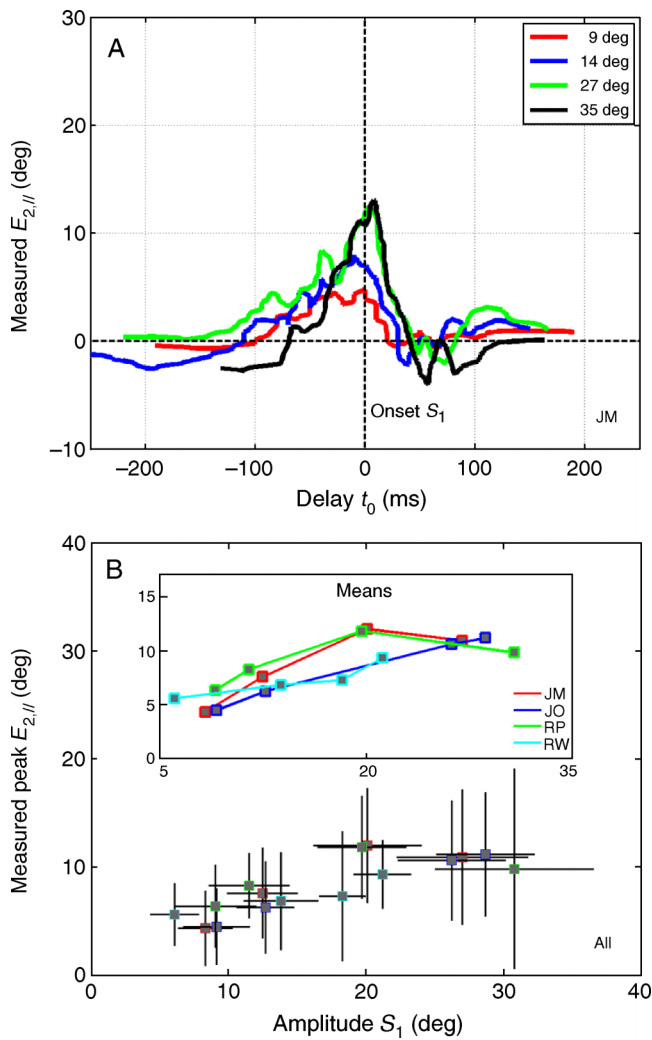


Figure 10. Dependence of perisaccadic localization errors on first-saccade amplitude. (A) Running averaged data from subject JM show a mild increase of peak errors with amplitude. (B) Data from all subjects. Bottom: mean and standard deviations. Inset: means connected. Errors saturate at about 10 deg amplitude.

measured (Figure 11A) and predicted (Figure 11B) residual errors for one of our subjects (JO).

We then subjected both data sets to the multiple linear regression analysis of Equation 19. As explained in the Methods section, we performed two regressions: The first regression was applied to the entire data set. Note, that in the predicted errors we did not incorporate an additional (hypothetical) undershoot. Thus, regression on the predicted residual errors should yield an insignificant contribution of motor error. Indeed, the predicted residual errors for long leads and delays are zero (Figure 11B).

Table 3 summarizes the results of the normalized multiple regression analysis performed on the entire $[-250, +250]$ ms interval of flash delays, for measured and predicted data sets. As expected, motor error does not contribute to the predicted errors, but it resulted in a strong negative contribution to the measured data. In

contrast, the saccade amplitude yielded a clear positive contribution to the model predictions, but the general effect appeared to be negligible, or even negative, for the measured data. Mean eye velocity did not appear to influence the overall error patterns in a consistent way, neither for the measured data nor for the predicted data. However, these parameters measure the average trends across the entire interval and therefore cannot capture more complex dynamics of the saccade kinematics during the flash delay.

Thus, a much more sensitive analysis is provided by the windowed regression analysis, illustrated in Figure 5B, in which the parameter values were estimated across systematically shifted time bins (100 ms wide, 90 ms overlap; see Methods section). Figure 12 (top) compares the results of this analysis for measured (Figure 12A) and predicted (Figure 12B) residual errors of one of our subjects (JM).

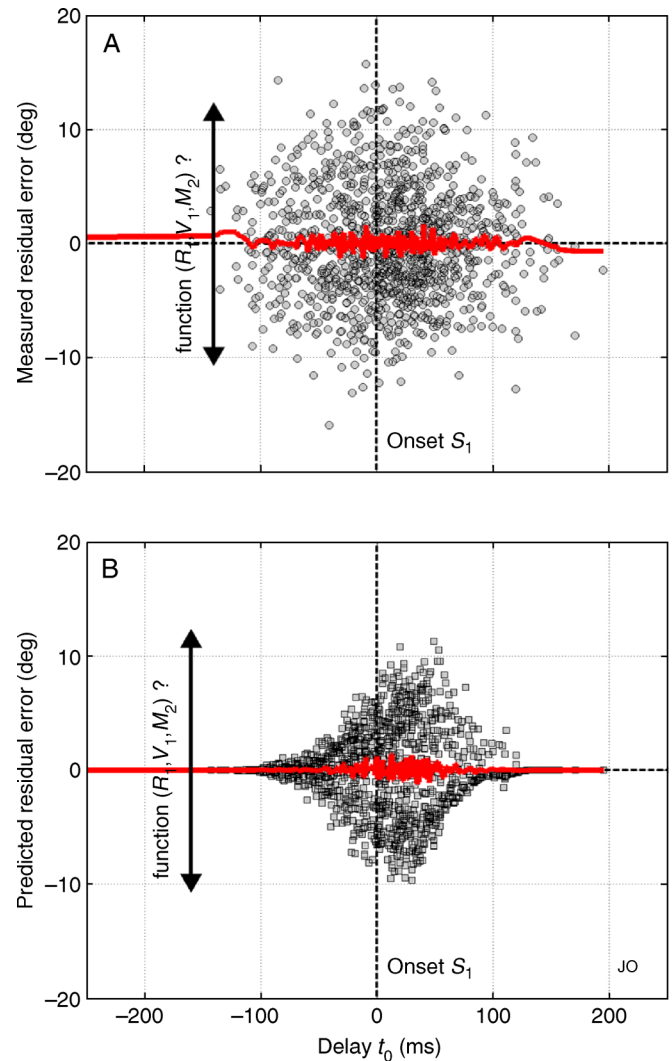


Figure 11. Residual errors for measured (A) and predicted (B) responses. Pooled responses (all amplitudes); data from subject JO. Predictions were based on the oculomotor model with default parameters.

	Data				Oculomotor model				<i>N</i>
	<i>a</i>	<i>b</i>	<i>c</i>	<i>r</i>	<i>a</i>	<i>b</i>	<i>c</i>	<i>r</i>	
JM	−0.29	−0.28	−0.26	0.30	0.86	−0.11	0.05	0.76	1031
JO	−0.08	0.13	−0.48	0.51	0.82	0.04	0.008	0.85	1177
RP	−0.45	0.28	−0.62	0.55	0.74	−0.04	−0.02	0.66	909
RW	0.04	−0.08	−0.84	0.82	0.80	0.006	0.06	0.76	626

Table 3. Results of multiple linear regression (Equation 19) on the residual errors of measured (left) and predicted (right) data across the entire flash-delay interval. Note consistent negative contribution of motor error (*c*) in the data and a large positive amplitude contribution (*a*) in the model predictions.

Clearly, the patterns between measurements and predictions for $a(t_0)$, $b(t_0)$, and $c(t_0)$ are very different. Like in Figure 5C for the simulated data, also for the actually measured saccades a single-peaked positive-only contribution of the primary-saccade amplitude is predicted to the perisaccadic localization errors. This amplitude function peaks during the primary saccade. In contrast, the influence

of mean eye velocity has a biphasic shape. A positive velocity coefficient is predicted prior to saccade onset, while the effect changes sign during the saccade. These predicted patterns remain when noise is added to the errors (see Supplemental Material). This feature explains why the regression on the entire interval failed to measure a contribution of mean eye velocity (Table 3).

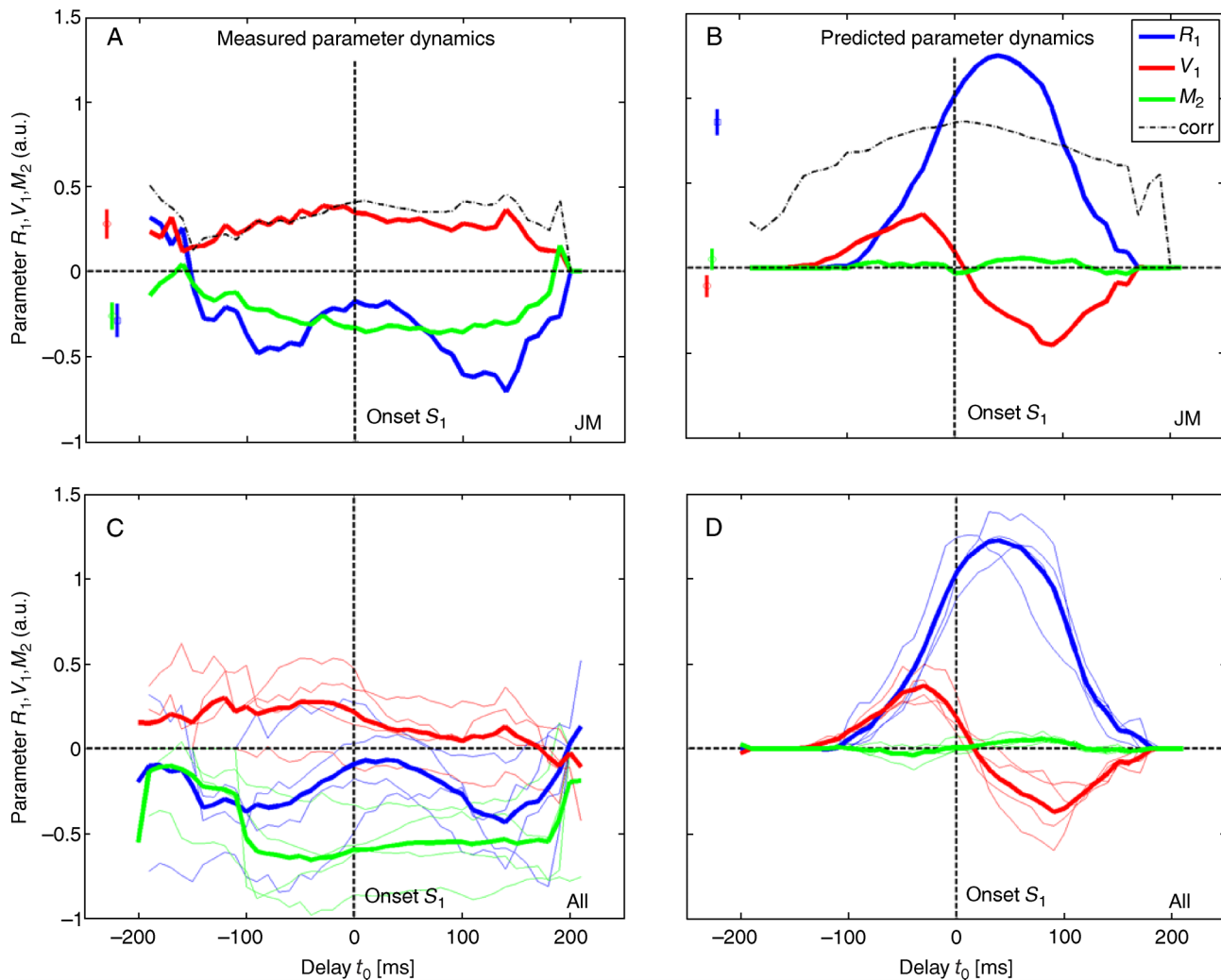


Figure 12. Parameter dynamics for measured (A, C) and predicted (B, D) responses. Same format as Figures 4C and 5. Predictions based on the oculomotor model with default parameters (see also Supplemental Material).

However, no such patterns were obtained for the measured data. As the partial correlation coefficient for mean eye velocity was not systematically modulated at all during the entire interval, the minor contribution of first-saccade amplitude appeared to scatter near zero, with a tendency to be even negative. Before and during the saccade, the amplitude parameter shows a slight increase. The contribution of the motor error was negative and roughly constant throughout the flash interval, which indicates that indeed the secondary saccades tended to undershoot the target flash in an amplitude-dependent way that was hardly influenced by the timing of the flash.

Figure 12 (bottom) shows the results of the dynamic regression analysis for all four subjects. Note that the predicted data (Figure 12D) yielded consistent results for all three partial correlation coefficients, whereas the measured error patterns (Figure 12C) did not contain any such systematic variation with stimulus delay. The contribution of primary-saccade amplitude tended to increase slightly during the saccade, which reflects the weak amplitude dependence of the peak localization errors shown in Figure 10.

Effect of stimulus duration on perisaccadic errors

In the duration paradigm, the second target was flashed for either 5, 15, or 50 ms. The first saccade was always horizontal (left/right) with an amplitude of 14 deg. Note that the different visuomotor feedback models do not predict a specific effect of stimulus duration on the perisaccadic localization errors. However, we found for all subjects that the 50-ms stimuli yielded the smallest localization errors. The results for the 5- and the 15-ms stimuli were not systematically different. Figure 13A shows the running average results for the three stimulus conditions of subject JM. Note that the peak localization error for the 50-ms stimuli decreased by nearly 50% and was shifted toward negative delays by almost 50 ms.

Optimal direction of perisaccadic errors

According to the various visuomotor feedback theories, the error vector of the second saccade, \vec{E}_2 (see Figure 2), is expected to be roughly parallel to the first-saccade response. Thus, the distribution of endpoints (which also includes other sources of error, like systematic undershoots, see Figure 2) should be elongated in the direction of the initial saccade. To test whether this is

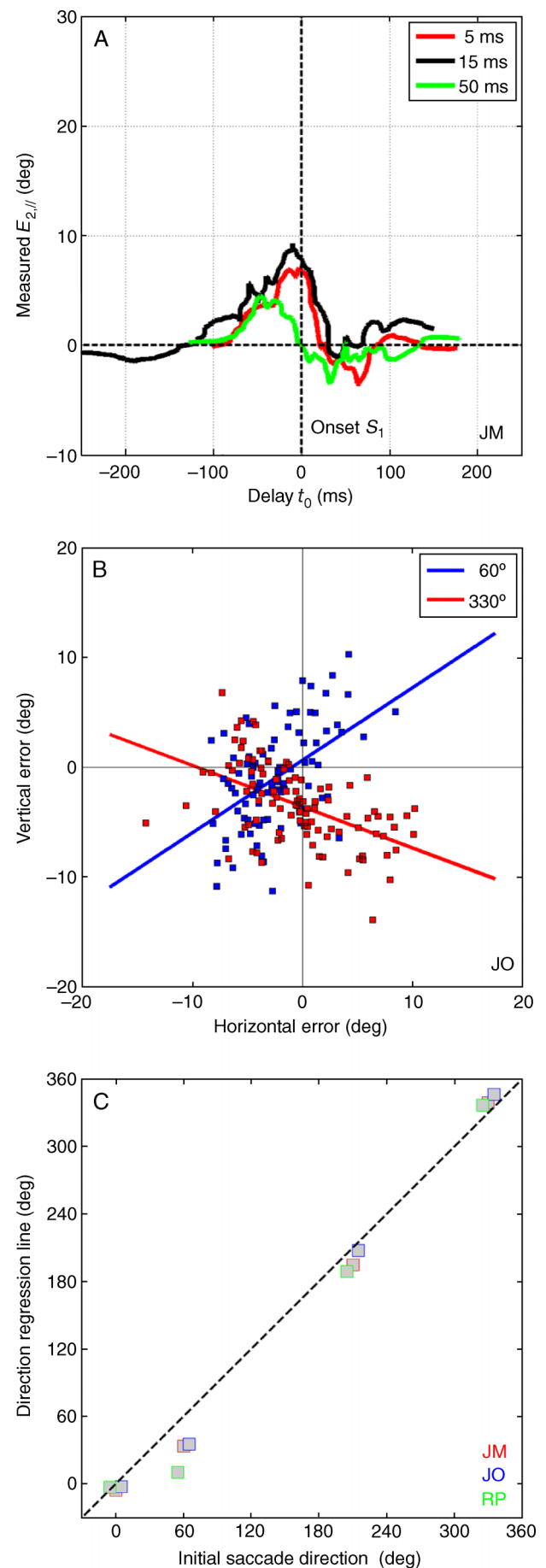


Figure 13. (A) Effect of flash duration on localization errors. (B) Errors are distributed along the direction of the first saccade, here shown for 60 and 330 deg. (C) Direction of regression lines for three subjects against initial saccade direction.

Direction	Regression	JM	JO	RP
[0, 180]	Slope	−0.13	−0.01	+0.03
	Bias	−0.47	−3.00	−2.20
	Corr	0.19	0.01	0.03
60	Slope	+0.58	+0.66	+0.27
	Bias	−0.01	+0.64	+0.19
	Corr	0.53	0.50	0.31
210	Slope	+0.42	+0.26	+0.25
	Bias	−1.70	−1.18	−2.70
	Corr	0.66	0.42	0.34
330	Slope	−0.34	−0.38	−0.33
	Bias	−0.78	−3.60	−1.53
	Corr	0.46	0.51	0.28

Table 4. Regression results $E_v = a + bE_h$ for the error vector (E_h , E_v) distributions for four different initial saccade directions and three subjects (Figure 13). The slopes of the regression lines tend to follow the initial saccade direction. The negative bias, obtained in most cases, reflects a systematic undershoot of the second saccade in the vertical direction.

indeed the case, we determined a linear regression line through the distribution of error endpoints for each initial saccade direction, for which we also included the data from the $[R_1, \Phi_1] = [14, 0]$ and $[14, 180]$ deg paradigm. Figure 13B shows the result of this analysis for the data of subject JO (directions +60 deg and 330 deg). In three subjects, we obtained qualitatively similar results. The results for the fourth subject (RW) were too noisy to yield meaningful regression lines and were therefore not included. Table 4 summarizes the results.

The slopes of the regression lines corresponded well to the directions of the initial saccade, indicating that the error vectors were on average aligned with the first-saccade response ($r = 0.995$, $N = 9$ sessions). This result is illustrated in Figure 13C.

Discussion

Summary

We have shown that existing models on visual-motor transformations predict that the amplitude and the kinematics of an intervening saccade systematically modulates the size of perisaccadic localization errors (Figures 4, 5, and 6). We specifically set out to test this prediction for the double-step saccade paradigm to briefly flashed point targets in darkness. Our analysis shows that perisaccadic mislocalizations are invariant to large variations of the saccade parameters (Figure 12). Our data therefore do not confirm the predictions of these models. We verified that the localization errors align with the direction of the intervening saccade (Figure 13B) and that increasing the

duration of the visual probe stimulus substantially reduces the errors (Figure 13A). We propose that the saccadic mislocalizations have a visual origin, and that apart from saccade direction, other saccade parameters have little effect. Thus, the oculomotor feedback signals, needed to update the retinal coordinates into an oculocentric motor error, are presumably accurate.

Related studies

Perisaccadic localization errors were first reported in a visual perceptual study by Matin and Pearce (1965) but have later also been observed in open-loop oculomotor studies in darkness. Dassonville et al. (1992) and Honda (1990, 1991) thus hypothesized that mislocalization around a saccade was not exclusively a perceptual illusion but also affected orienting behavior. The same underlying mechanism might therefore underlie both perceptual and behavioral mislocalizations. A sluggish eye-movement efference copy to update the retinal target coordinates could well explain the error patterns. Interestingly, Hallett and Lightstone (1976) reported accurate saccades in the double-step paradigm, and Dassonville et al. (1995) suggested that the apparent discrepancy in results might partially be explained by the presence or the absence of potential allocentric visual cues that could occur when double-step targets are presented in close spatial-temporal proximity. Yet, substantial variation of the gap interval between the targets had a relatively small effect on the errors (Dassonville et al., 1995).

Indeed, also studies in which visual references were intentionally present reported perisaccadic localization errors, albeit that the nature of the error patterns varied with the specifics of the testing conditions. Cai et al. (1997) employed a vernier alignment test and observed that the perceived location of a briefly (4 ms) flashed dot, relative to two vertically surrounding dots, appeared displaced in the direction of the saccade. However, the perceived displacement only occurred when the central dot was flashed separately within 100 ms before saccade onset, but it was absent when the three dots were flashed together. Since these experiments measured perceived relative displacements, it is unclear whether the localization errors followed similar patterns as in the double-step paradigm. Ross et al. (1997) reported that localization errors of a bar flashed around a saccade could be described by a nonuniform compression of visual space around the saccade onset, in combination with a sluggish eye-position signal. Awater and Lappe (2006) and Lappe et al. (2000) provided evidence that this nonuniform visual compression is due to postsaccadic visual processing because it required the presence of a postsaccadic visual reference (like e.g., a ruler). They explained their results by a two-stage model of visual-spatial perception, reminiscent to the saccade-target idea proposed by Bridgeman et al. (1994) and Deubel et al. (1998). In the

first stage, retinocentric and allocentric cues of the target display encode the relative locations of visual targets prior to the saccade. In the subsequent stage, these encoded cues are compared immediately after the saccade, in combination with eye-movement feedback. The weights of the different cues depend on the visual conditions, such as the presence or the absence of visual references, or on task demands that may modulate visual–spatial attention.

The only other study so far that has investigated the potential influence of the saccade parameters on perisaccadic mislocalization is by Ostendorf et al. (2007). In particular, that study looked at the relation between intersubject variation of peak saccade velocity and the amount of perceived visual compression. They found a correlation between the reported compression and a subject's saccade velocity, but not with other parameters, like saccade amplitude or latency.

Interestingly, perisaccadic mislocalization itself was not related to any of the saccade parameters. Although their analysis was performed on intersubject differences rather than on the entire repertoire of saccade variability within a subject, as reported here, this latter finding is nicely in line with our results (e.g., Figures 12A and 12C). The absence of a correlation for saccade amplitude in their study, however, could also be due to the small range of saccade amplitudes, as all their responses were evoked by a 10-deg target displacement. Ostendorf et al. (2007) concluded, in agreement with Awater and Lappe (2006), that perisaccadic mislocalization and visual compression are probably governed by different neural mechanisms.

In our experiments, we eliminated potential allocentric references to force the visuomotor system to rely on absolute retinal and extraretinal inputs. Thus, according to the two-stage model, the encoding stage could only use absolute retinal cues, as targets were temporally and spatially dissociated, whereas the second stage could only rely on eye-movement feedback, as postsaccadic visual cues were absent (open-loop conditions). Thus, visual compression might not be perceived in our experiments. Yet, our results suggest that in the presaccadic epoch eye-movement preparation influences the perceived direction of the visual target. Thus, it appears that the encoding stage does not only incorporate visual–spatial relationships.

Vliegen et al. (2005) measured head-free gaze shifts to double-step stimuli, in which a 50-ms target flash occurred around the first gaze shift. They did not find the systematic localization errors in the presaccadic epoch that would be expected from sluggish efferent feedback. Also when the second target was a brief auditory stimulus, localization was equally accurate for all target delays (Vliegen et al., 2004). Although it cannot be excluded that under head-unrestrained conditions the efference copies are more reliable than under head-restrained situations, these studies further support our conclusion that perisaccadic mislocalizations have a visual, rather than an oculomotor,

origin. In line with this hypothesis, Binda et al. (2007) recently demonstrated that when auditory and visual stimuli are presented together, perisaccadic localization errors nearly disappear. They hypothesized that the brain accounts for the unreliability of visual information in the presaccadic epoch, by allowing the auditory spatial information a stronger influence on target localization (Binda et al., 2007). A similar statistical argument has been proposed by Niemeier, Crawford, and Tweed (2003). Due to the inherent uncertainties in the oculomotor and the sensory signals, systematic mislocalizations could result from optimal inference. They showed that this principle could well account for the perceptual blindness of visual target displacement around the onset of saccades.

Implications for models

As described in the [Introduction](#) section, and shown in our simulations, the oculomotor feedback model (Dassonville et al., 1992, 1995; Honda, 1990, 1991), the visual dispersion and visuomotor models (Pola, 2004), and also the visual compression model (Ross et al., 1997) yield equivalent predictions for the behavior of perisaccadic mislocalizations as function of the first-saccade properties. The models also predict that slow and fast saccades of the same amplitude generate different errors for a given flash delay and that the influence of these saccade parameters varies in a nonlinear way during the flash interval.

Our experimental results show that the localization errors are largely insensitive to substantial variations in the first-saccade metrics and kinematics (Figure 12). Only for the smallest saccades the errors tended to decrease slightly (Figure 10), but we observed no systematic effect of the saccade kinematics (Figure 12). None of the models, discussed so far, account for this discrepancy, unless one adopts the unlikely assumption that the filter and delay parameters depend in a complex way on the eccentricity of the first visual target.

Taken together, the conceptual framework of visuomotor transformations, expressed by [Equation 2](#), suggests that the localization errors obtained in the double-step experiment may have a visual, rather than an oculomotor, origin. However, the visual dispersion model of Pola (2004) does not predict the correct behavior either, as its predictions are indistinguishable from the other three models described in the [Introduction](#) and in the [Methods](#) section. Thus, we propose that the retinal signal undergoes a *spatial*, rather than a temporal distortion.

Figure 14 presents a simple heuristic model that could account for our data. In the period during saccade preparation, the retinal representation of the visual stimulus is transiently shifted in the direction of the saccade vector. The shift, β , depends on the stimulus delay relative to the saccade, which represents the transient influence of the oculomotor system on visual processing,

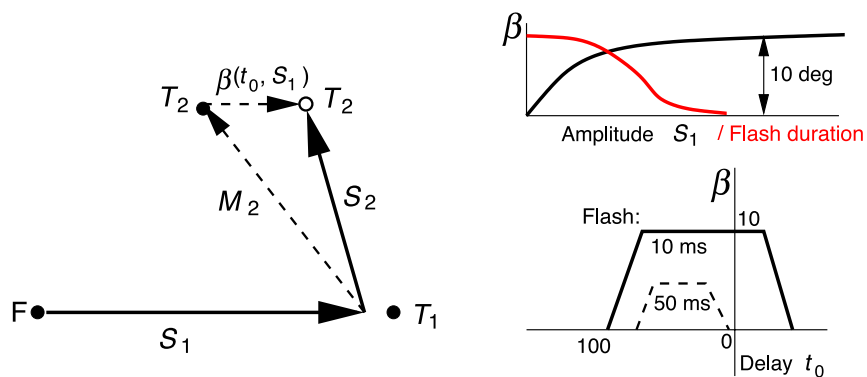


Figure 14. Heuristic model that explains perisaccadic localization errors in the double-step paradigm. A perceived uniform visual shift, β , of the target around saccade onset depends on saccade amplitude (top, black) but diminishes with increasing duration of the target (red). The maximum size of the effect is about 10 deg.

and also on visual factors like stimulus duration, D_2 , the presence or absence of visual references, or on task demands. The shift depends also on the saccade amplitude, S_1 (Figure 10B), but saturates at about 10 deg:

$$\begin{aligned} \vec{R}_2^p &= \vec{R}_2 + \beta(t_0, D_2, S_1) \cdot \hat{s}_1 \\ \vec{T}_2^p &= \vec{R}_2^p - \Delta \vec{S}_1, \end{aligned} \quad (20)$$

with \hat{s}_1 the unit vector along the saccade.

For very small saccades (e.g., microsaccades during fixation), the oculomotor influence on the visual representation is minimal, which accounts for the absence of localization errors during fixation (Awater & Lappe, 2006; Cai et al., 1997). The size of the effect also decreases rapidly with increasing stimulus duration (Figure 13A). The internal representation of eye position, however, is considered to be accurate, so that the spatial mislocalization of targets is entirely due to transient visual factors. In a recent behavioral study with monkeys, probe durations of 100 ms were used, in which case the errors were predominantly negative (i.e., against the direction of the saccade; Jeffries, Kusunoki, Bisley, Cohen, & Goldberg, 2007). Error reversals in human subjects have also been observed by Honda (1991). To accommodate for this latter effect (which was not systematically present in our own data), the transient shift in the model, $\beta(t_0)$, should be given a negative tail for positive delays. The predominantly negative errors observed in monkeys, however, may possibly be caused by the longer stimulus durations. At this stage, however, it is not possible to extrapolate our own findings (maximum durations of 50 ms) to longer probe durations, and we have not attempted to adjust the simple model of Equation 20 to a wider range of stimulus properties.

To test the predictions of this simple model, we simulated 500 saccades with Equations 14, and 15, in the same way as shown in Figures 4, 5, and 6. The result of this simulation is shown in Figure 15. The error patterns depend slightly on the saccade amplitude, due to

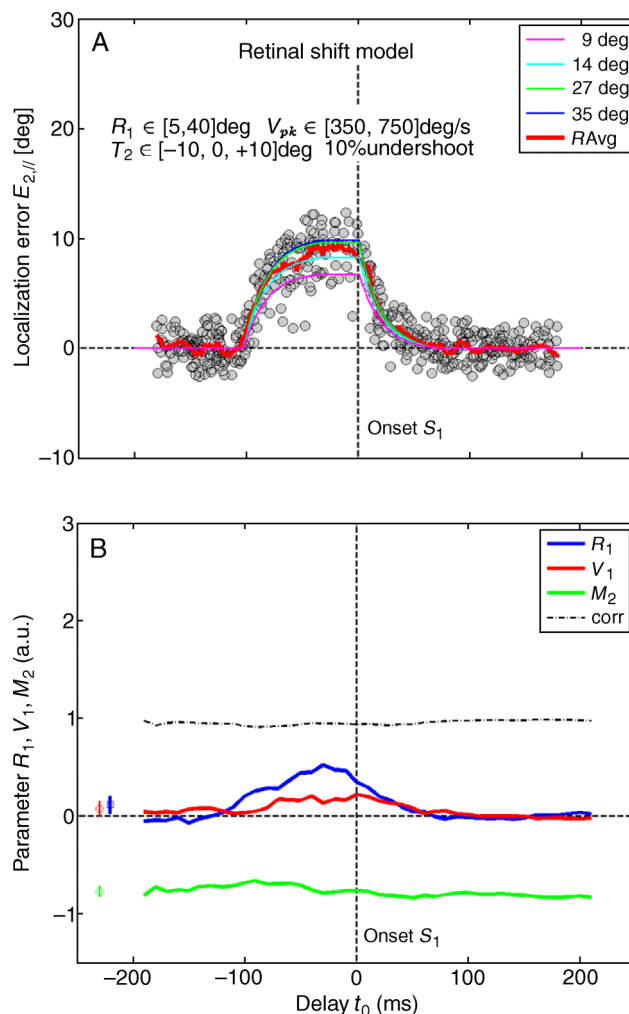


Figure 15. Results of simulations for 500 randomly selected first saccades with the retinal shift model. (A) Error patterns around saccade onset. Running averages for saccades of different amplitudes are indicated in color. The red curve is the grand running average through all the data. (B) Parameter dynamics follow qualitatively the results shown in Figure 11C.

the saturating influence of the oculomotor programming stage on the retinal shift. However, in our model, this influence has no dynamics. The parameters of the multiple regression analysis (Equation 19) therefore only show a mild positive influence of saccade amplitude and a strong negative but constant influence of the motor error. These simulated data resemble the measured regression results shown in Figure 12C quite well.

Neural mechanisms

Oculomotor signals have been shown to influence visual receptive fields in cortical and subcortical areas by different neural mechanisms. For example, multiplicative gain fields were first described for visual receptive fields of cells in the posterior parietal cortex (Andersen, Essick, & Siegel, 1985). Such cells modulate their visual spatial tuning curve with static changes in eye position. As these cells do not respond to eye position changes in the absence of a visual stimulus in their receptive field, the effect is multiplicative rather than additive. In later studies, similar eye-position modulations have been reported for saccade-related cells in the midbrain superior colliculus (Van Opstal, Hepp, Suzuki, & Henn, 1995) for visual receptive fields in the primary visual cortex (Weyand & Malpeli, 1993) and even on the tonotopic tuning curves of auditory cells in the monkey inferior colliculus (Zwiers, Versnel, & Van Opstal, 2004). Oculomotor gain fields have been proposed to mediate the transformation of retinal coordinates into a head-centered reference frame (Zipser & Andersen, 1988), or vice versa, from a head-centered acoustic reference frame into an oculocentric reference frame (Zwiers et al., 2004). Yet, the dynamics of such a putative transformation have not been studied so far. It is therefore unclear how and whether oculomotor gain fields could underlie either perisaccadic mislocalization or visual compression.

An alternative mechanism related to visuomotor transformations is predictive remapping. In cells that show this phenomenon, visual receptive fields shift already *prior* to the saccade onset in a direction that compensates for the future visual consequences of the saccade. Predictive remapping has been demonstrated in the responses of cells within several cortical and subcortical saccade-related regions: posterior parietal cortex (Duhamel et al., 1992), frontal eye fields (Umeno & Goldberg, 1997), and superior colliculus (Walker et al., 1995). Predictive shifts of visual receptive fields have also been observed in regions involved in visual object processing and visual attention, like area V4 (Tolias et al., 2001).

Thus, considering the transient nature of perisaccadic localization errors, predictive remapping might be a better candidate for a neural correlate of localization errors than static eye-position gain fields. In predictive remapping, receptive fields shift in a direction that opposes the saccade ($T_E^{\text{PRED}} = R_1 - S_1$). Thus, perisaccadic errors in

the saccade direction could emerge when either feedback about eye displacement would fall short of the actual saccade, or when the retinal representation of the target would transiently shift in the saccade direction.

Recent evidence has indicated that the superior colliculus provides the efference copy signal that could underlie the dynamic shifts in the visual receptive fields of frontal eye-field cells (Sommer & Wurtz, 2006). Moreover, a detailed analysis of the firing behavior of SC cells has indicated that their population activity faithfully reflects the amplitude and kinematics of the planned saccadic eye movement (Goossens & Van Opstal, 2006). This efferent feedback mechanism could therefore provide the kinematically accurate displacement information needed to implement the correct transformation. Neurophysiological evidence also suggests that the dynamics of visual-receptive field shifts in parietal cells might be linked to perisaccadic localization errors, as neurons respond to stimuli presented in both the original and the future receptive field during the perisaccadic interval. This mechanism therefore effectively increases the size of the receptive field in the saccade direction (Kusunoki & Goldberg, 2003). Whether this effect can be quantitatively connected to the measured mislocalization patterns, however, is still unclear.

According to the simple model of Figure 14, the oculomotor feedback signal is assumed to be accurate, but the retinal representation transiently shifts in the saccade direction. Recently, Krekelberg, Kubischik, Hoffmann, and Bremmer (2003) have described responses in visual motion areas MT and MST to bars flashed for 8 ms around the onset of a saccade. An ideal observer analysis on the cell responses suggested that the visual information transmitted by these cells could reflect perisaccadic mislocalizations in a retinocentric reference frame, as the cells appeared to be transiently “confused” around the saccade event. The size of the inferred errors (about 5 deg) was in the same order of magnitude as reported in our study.

It would be interesting to test whether the visual confusion in MT/MST cells, or the expansion of visual receptive fields in parietal cells, is influenced by the duration of the target flash, and whether it is invariant to the variability in the saccades.

Acknowledgments

We thank Christiaan Taris for his participation in the data collection and analysis. We also thank Hans Kleijnen and Stijn Martens for valuable technical assistance and our naive subjects JM, RW, and RP who kindly participated numerous times in these experiments. This research was funded by the Netherlands Organization for Scientific Research, NWO, project grants 812.07.005

ALW (SVW), 805.05.003 ALW/VICI, (AJVO, SVW), and by the Radboud University Nijmegen (AJVO).

Commercial relationships: none.

Corresponding author: John Van Opstal.

Email: j.vanopstal@science.ru.nl.

Address: Department of Biophysics, Geert Grooteplein 21, 6525 EZ Nijmegen, The Netherlands.

Footnote

¹Equations 12 and 13 were adopted from Ross et al. (1997), but here the equations express the visual targets in *oculocentric* rather than in *head-centered* coordinates. Further, the extraretinal signal represents relative eye displacements rather than absolute eye positions. We also noted two errors in their original equations: (i) the extraretinal on- and offset profiles should be normalized by a factor $(\sigma_{0,1}\sqrt{2\pi})^{-1}$, and (ii) the argument of the exponent of $C(T, t)$ should be dimensionless, hence the factor S_1^2 instead of S_1 .

References

- Andersen, R. A., Essick, G. K., & Siegel, R. M. (1985). Encoding of spatial location by posterior parietal neurons. *Science*, *230*, 456–458. [[PubMed](#)]
- Awater, H., Burr, D., Lappe, M., Morrone, M. C., & Goldberg, M. E. (2005). Effect of saccadic adaptation on localization of visual targets. *Journal of Neurophysiology*, *93*, 3605–3614. [[PubMed](#)] [[Article](#)]
- Awater, H., & Lappe, M. (2006). Mislocalization of perceived saccade target position induced by perisaccadic visual stimulation. *Journal of Neuroscience*, *26*, 12–20. [[PubMed](#)] [[Article](#)]
- Binda, P., Bruno, A., Burr, D. C., & Morrone, M. C. (2007). Fusion of visual and auditory stimuli during saccades: A Bayesian explanation for perisaccadic distortions. *Journal of Neuroscience*, *27*, 8525–8532. [[PubMed](#)] [[Article](#)]
- Bridgeman, B., Van der Heijden, A. H. C., & Velichkovsky, B. M. (1994). A theory of visual stability across saccadic eye movements. *Behavioral and Brain Sciences*, *17*, 247–292.
- Cai, R. H., Pouget, A., Schlag-Rey, M., & Schlag, J. (1997). Perceived geometrical relationships affected by eye-movement signals. *Nature*, *386*, 601–604. [[PubMed](#)]
- Collewijn, H., van der Mark, F., & Jansen, T. C. (1975). Precise recording of human eye movements. *Vision Research*, *15*, 447–450. [[PubMed](#)]
- Dassonville, P., Schlag, J., & Schlag-Rey, M. (1992). Oculomotor localization relies on a damped representation of saccadic eye displacement in human and nonhuman primates. *Visual Neuroscience*, *9*, 261–269. [[PubMed](#)]
- Dassonville, P., Schlag, J., & Schlag-Rey, M. (1995). The use of egocentric and exocentric location cues in saccadic programming. *Vision Research*, *35*, 2191–2199. [[PubMed](#)]
- Deubel, H., Bridgeman, B., & Schneider, W. X. (1998). Immediate post-saccadic information mediates space constancy. *Vision Research*, *38*, 3147–3159. [[PubMed](#)]
- Duhamel, J. R., Colby, C. L., & Goldberg, M. E. (1992). The updating of the representation of visual space in parietal cortex by intended eye movements. *Science*, *255*, 90–92. [[PubMed](#)]
- Goossens, H. H., & Van Opstal, A. J. (2006). Dynamic ensemble coding of saccades in the monkey superior colliculus. *Journal of Neurophysiology*, *95*, 2326–2341. [[PubMed](#)] [[Article](#)]
- Hallett, P. E., & Lightstone, A. D. (1976). Saccadic eye movements toward stimuli triggered by prior saccades. *Vision Research*, *16*, 99–106. [[PubMed](#)]
- Honda, H. (1990). Eye movements to a visual stimulus flashed before, during, or after a saccade. In M. Jeannerod & N. J. Hillsdale (Eds.), *Attention and performance* (vol. 13, pp. 567–582). Hillsdale: Erlbaum.
- Honda, H. (1991). The time course of visual mislocalization and of extraretinal eye position signals at the time of vertical saccades. *Vision Research*, *31*, 1915–1921. [[PubMed](#)]
- Jeffries, S. M., Kusunoki, M., Bisley, J. W., Cohen, I. S., & Goldberg, M. E. (2007). Rhesus monkeys mislocalize saccade targets flashed for 100 ms around the time of a saccade. *Vision Research*, *47*, 1924–1934. [[PubMed](#)]
- Jürgens, R., Becker, W., & Kornhuber, H. H. (1981). Natural and drug-induced variations of velocity and duration of human saccadic eye movements: Evidence for a control of the neural pulse generator by local feedback. *Biological Cybernetics*, *39*, 87–96. [[PubMed](#)]
- Krekelberg, B., Kubischik, M., Hoffmann, K. P., & Bremmer, B. (2003). Neural correlates of visual localization and perisaccadic mislocalization. *Neuron*, *37*, 537–545. [[PubMed](#)] [[Article](#)]
- Kusunoki, M., & Goldberg, M. E. (2003). The time course of perisaccadic receptive field shifts in the lateral intraparietal area of the monkey. *Journal of Neurophysiology*, *89*, 1519–1527. [[PubMed](#)] [[Article](#)]
- Lappe, M., Awater, H., & Krekelberg, B. (2000). Postsaccadic visual references generate presaccadic

- compression of space. *Nature*, 403, 892–895. [[PubMed](#)]
- Matin, L., & Pearce, D. G. (1965). Visual perception of direction for stimuli flashed during voluntary saccadic eye movement. *Science*, 148, 1485–1488. [[PubMed](#)]
- Niemeier, M., Crawford, J. D., & Tweed, D. B. (2003). Optimal transsaccadic integration explains distorted spatial perception. *Nature*, 422, 76–80. [[PubMed](#)]
- Ostendorf, F., Fischer, C., Finke, C., & Ploner, C. J. (2007). Perisaccadic compression correlates with saccadic peak velocity: Differential association of eye movement dynamics with perceptual mislocalization patterns. *Journal of Neuroscience*, 27, 7559–7563. [[PubMed](#)] [[Article](#)]
- Pola, J. (2004). Models of the mechanisms underlying perceived location of a perisaccadic flash. *Vision Research*, 44, 2799–2813. [[PubMed](#)]
- Robinson, D. A. (1963). A method of measuring eye movement using a scleral search coil in a magnetic field. *IEEE Transactions on Biomedical Engineering*, 10, 137–145. [[PubMed](#)]
- Ross, J., Morrone, M. C., & Burr, D. C. (1997). Compression of visual space before saccades. *Nature*, 386, 598–601. [[PubMed](#)]
- Schlag, J., & Schlag-Rey, M. (2002). Through the eye, slowly: Delays and localization errors in the visual system. *Nature Reviews, Neuroscience*, 3, 191–215. [[PubMed](#)]
- Scudder, C. A. (1988). A new local feedback model of the saccadic burst generator. *Journal of Neurophysiology*, 59, 1455–1475. [[PubMed](#)]
- Sommer, M. A., & Wurtz, R. H. (2002). A pathway in primate brain for internal monitoring of movements. *Science*, 296, 1480–1482. [[PubMed](#)]
- Sommer, M. A., & Wurtz, R. H. (2006). Influence of the thalamus on spatial visual processing in frontal cortex. *Nature*, 444, 374–377. [[PubMed](#)]
- Sparks, D. L., & Mays, L. E. (1983). Spatial localization of saccade targets. I. Compensation for stimulation-induced perturbations in eye position. *Journal of Neurophysiology*, 49, 45–63. [[PubMed](#)]
- Sparks, D. L., & Porter, J. D. (1983). Spatial localization of saccade targets. II: Activity of superior colliculus neurons preceding compensatory saccades. *Journal of Neurophysiology*, 49, 64–74. [[PubMed](#)]
- Tolias, A. S., Moore, T., Smirnakis, S. M., Tehovnik, E. J., Siapas, A. G., & Schiller, P. H. (2001). Eye movements modulate visual receptive fields of V4 neurons. *Neuron*, 29, 757–767. [[PubMed](#)] [[Article](#)]
- Umeno, M. M., & Goldberg, M. E. (1997). Spatial processing in the monkey frontal eye field. I. Predictive visual responses. *Journal of Neurophysiology*, 78, 1373–1383. [[PubMed](#)] [[Article](#)]
- Van Gisbergen, J. A., Robinson, D. A., & Gielen, S. (1981). A quantitative analysis of generation of saccadic eye movements by burst neurons. *Journal of Neurophysiology*, 45, 417–442. [[PubMed](#)]
- Van Opstal, A. J., Hepp, K., Suzuki, Y., & Henn, V. (1995). Influence of eye position on activity in monkey superior colliculus. *Journal of Neurophysiology*, 74, 1593–1610. [[PubMed](#)]
- Vliegen, J., Van Grootel, T. J., & Van Opstal, A. J. (2004). Dynamic sound localization during rapid eye-head gaze shifts. *Journal of Neuroscience*, 24, 9291–9302. [[PubMed](#)] [[Article](#)]
- Vliegen, J., Van Grootel, T. J., & Van Opstal, A. J. (2005). Gaze orienting in dynamic visual double steps. *Journal of Neurophysiology*, 94, 4300–4313. [[PubMed](#)] [[Article](#)]
- Von Helmholtz, H. (1866). *Handbuch der physiologische optik*. Leipzig, Voss.
- Walker, M. F., Fitzgibbon, E. J., & Goldberg, M. E. (1995). Neurons in the monkey superior colliculus predict the visual result of impending saccadic eye movements. *Journal of Neurophysiology*, 73, 1988–2003. [[PubMed](#)]
- Weyand, T. G., & Malpeli, J. G. (1993). Responses of neurons in primary visual cortex are modulated by eye position. *Journal of Neurophysiology*, 69, 2258–2260. [[PubMed](#)]
- Zipser, D., & Andersen, R. A. (1988). A back-propagation programmed network that simulates response properties of a subset of posterior parietal neurons. *Nature*, 331, 679–684. [[PubMed](#)]
- Zwiers, M. P., Versnel, H., & Van Opstal, A. J. (2004). Involvement of monkey inferior colliculus in spatial hearing. *Journal of Neuroscience*, 24, 4145–4156. [[PubMed](#)] [[Article](#)]